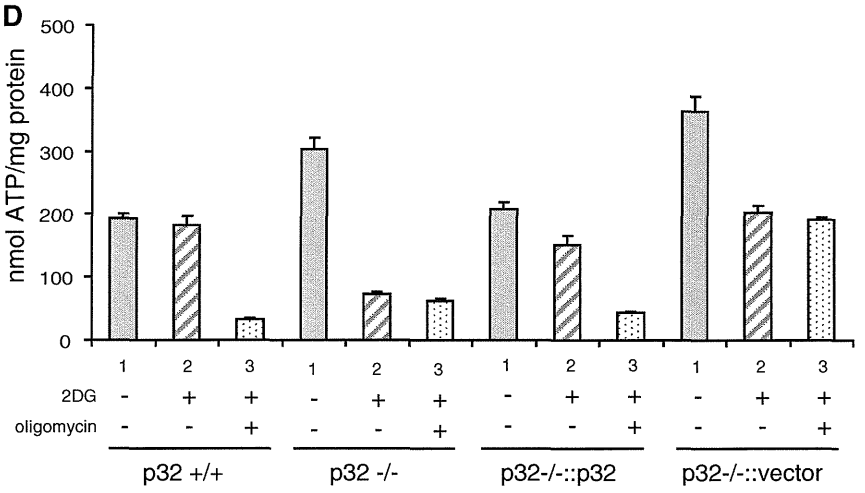

	p32 +/+	p32 -/-	p32 -/- :: p32	p32 -/- :: vector
Total ATP(lane1)	387.7	607.4	417.0	725.4
Glycolysis ATP(lane1-2)	23.9	462.2	114.6	320.9
Mitochondrial ATP(lane2-3)	297.6	20.6	213.5	20.8

(nmol ATP/mg protein)

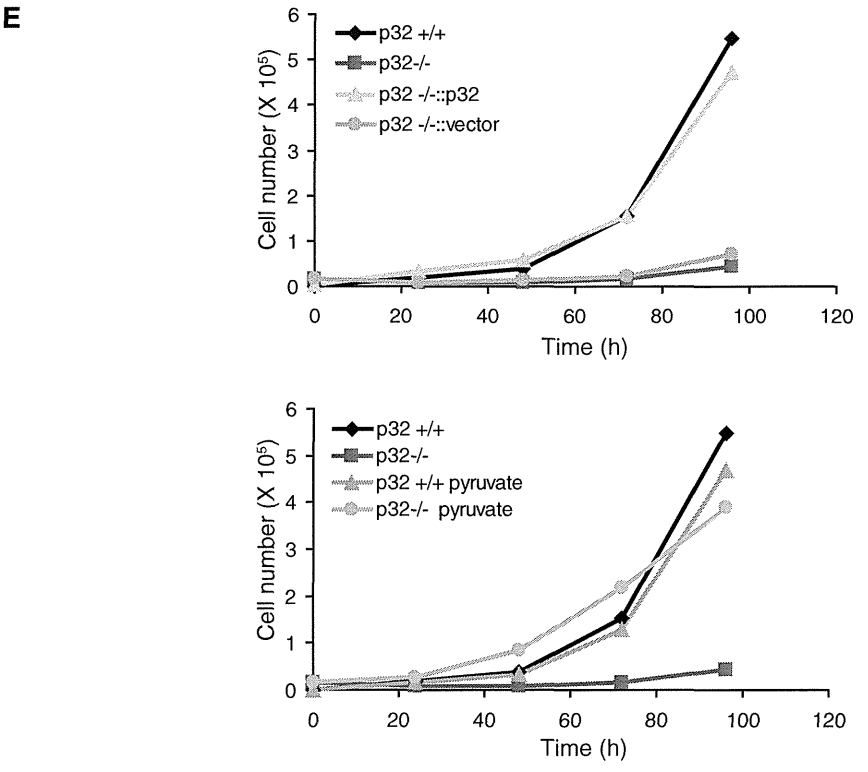

Figure 2. Continued

(**D**) Effects of 2-deoxy-D-glucose (2DG) (20 mM) and oligomycin (10 μM) on intracellular ATP content in MEFs. The ATP content in untreated MEFs is presented in lane 1. The ATP concentration of untreated MEFs (lane 1) was subtracted from that of 2DG-treated MEFs (lane 2) for assessment of glycolytic ATP production (lanes 1 and 2). The ATP concentration in 2DG-treated cells (lane 2) was subtracted from that in cells treated with 2DG + oligomycin (lane 3) for mitochondrial ATP production (lanes 2–3). Wild-type ($p32^{+/+}$), p32-knockout ($p32^{-/-}$), re-expressed p32 ($p32^{-/-}$::*p32*) and vector only-transfected ($p32^{-/-}$::vector) MEFs were used. The ATP response was measured using a Luminescence ATP assay kit in a 96-well plate. Data show the mean ± SD of triplicate experiments. (**E**) Cell proliferation monitored in MEFs. Upper panel: the diamonds, squares, triangles and circles represent wild-type MEFs ($p32^{+/+}$), p32-knockout MEFs ($p32^{-/-}$), knockout MEFs with reintroduced *p32* cDNA ($p32^{-/-}$::*p32*) and knockout MEFs with introduced vector-only cDNA ($p32^{-/-}$::vector), respectively. Lower panel: pyruvate (1 mM) was added to wild-type and $p32^{-/-}$ MEFs. The cell number was counted at 24, 48, 72 and 96 h after seeding. Here, we used DMEM (1000 mg/l glucose) supplemented with 10% dialyzed FBS without pyruvate.

proliferation (data not shown). Taken together with no decrease of cellular ATP in $p32^{-/-}$ MEFs (Figure 2D), these results suggest that impaired regeneration of NAD^+ (probably by complex I) is particularly critical for the retardation of $p32^{-/-}$ MEF proliferation.

No decreased mtDNA copy number and RNA expression

We measured the mtDNA copy number because the observed defects were likely related to mtDNA. The normal copy number of mtDNA was confirmed by qPCR, which excluded defects of mtDNA replication and/or repair as a cause of compromised protein synthesis (Figure 3A). To determine whether p32 affected the transcription of mtDNA, total RNA was isolated from cells and was assessed by qRT–PCR (Figure 3B). The steady-state level of 12S and 16S rRNA did not show a significant change between wild-type and $p32^{-/-}$ MEFs. No mtDNA-encoded mRNAs showed a decrease in p32-knockout MEFs compared with those in wild-type cells, although the levels of *ND1* and *ND6* transcripts were increased two-fold in knockout cells. The RNA expression levels in p32-re-expressed cells were also not significantly changed compared with those in wild-type cells (Figure 3B). Thus, p32 knockout did not cause a decrease in mtDNA-encoded transcripts. These results suggest that p32 deficiency does not affect the amounts of mtDNA or mRNAs.

Knockout of p32 decreases mitochondria- and nuclear-encoded proteins in mitochondria

mtDNA encodes 13 polypeptides/subunits of the mitochondrial electron respiratory chain. To determine why depletion of p32 caused a respiratory defect, we measured the expression of several members of the

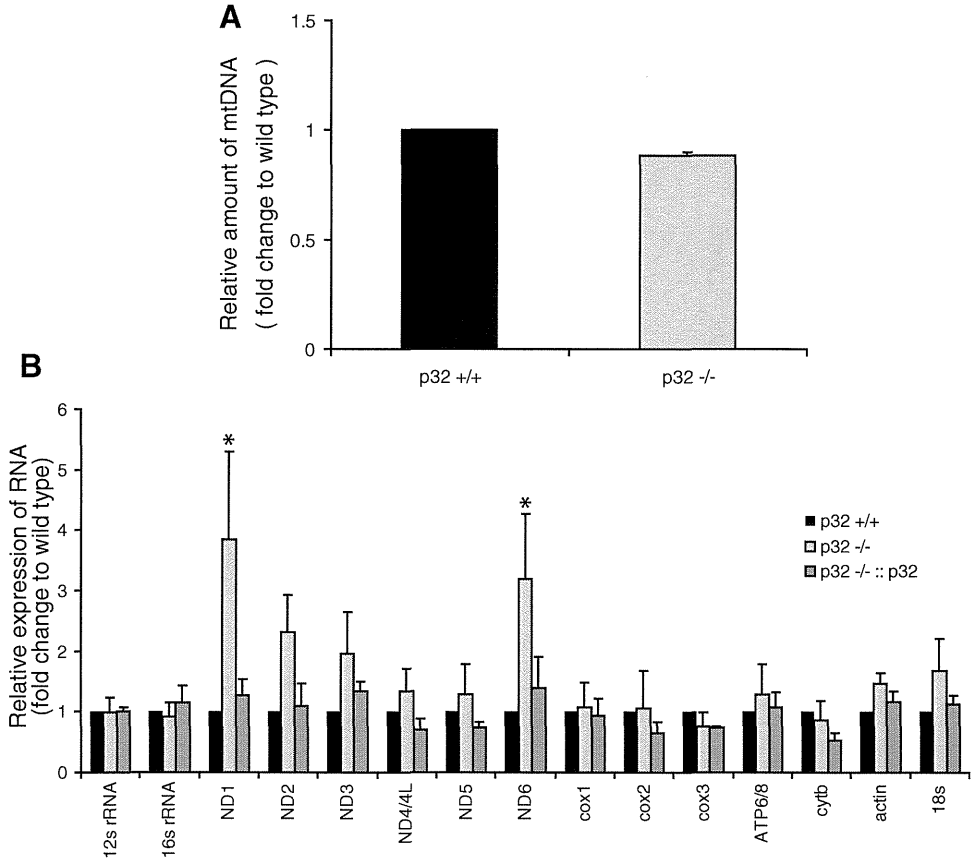

Figure 3. MtDNA copy number, RNA and protein expression in $p32^{-/-}$ MEFs. (**A**) The amount of mtDNA per cell was estimated based on the ratio of mtDNA/nuclear (n)DNA (ND2/AT-III). The relative mtDNA amount between $p32^{-/-}$ and $p32^{+/+}$ cells is shown. (**B**) Real-time PCR quantification of mitochondrial gene transcript levels isolated from wild-type ($p32^{+/+}$) MEFs, p32-knockout ($p32^{-/-}$) MEFs, and knockout MEFs with reintroduced *p32* cDNA ($p32^{-/-}$::*p32*). Two nuclear-encoded RNA species (*β-actin* and *18S* rRNA) were also quantified. Data were normalized to the expression level in wild-type $p32^{+/+}$ MEFs for each RNA species. Data show the mean ± SD of triplicate experiments and $*P < 0.05$; versus controls ($p32^{+/+}$ versus $p32^{-/-}$). (**C**) Expression of mitochondrial proteins. Crude mitochondria were prepared from equal amounts of MEFs. Ten micrograms of protein for each sample was loaded. Blots were incubated with the indicated antibodies. Lane 1, wild-type MEFs; lane 2, p32-knockout MEFs; lane 3, knockout MEFs with reintroduced *p32* cDNA; lane 4, knockout MEFs with introduced vector-only cDNA. Mt: OXPHOS protein encoded by mitochondria DNA; N: OXPHOS protein encoded by the nucleus. (**D**) *In vivo* mitochondrial translation was performed for 60 min using the cell lysates. The products were labeled during the reaction with a mixture of [^{35}S]-methionine and [^{35}S]-cysteine in the presence of emetine and/or chloramphenicol, and then detected by autoradiography after SDS–PAGE (upper panel). Deficient translation was observed in p32-knockout cells (lane 3). Equal loading was confirmed by CBB staining following exposure (lower panel). Lanes 1 and 2, wild-type MEFs; lane 3, p32-knockout MEFs; lane 4, knockout MEFs with reintroduced *p32* cDNA; lane5, knockout MEFs with introduced p32::K89A/K93A mutant; lane 6, knockout MEFs with vector-only cDNA. The protein indicated are representative proteins based on their molecular weight.

(continued)

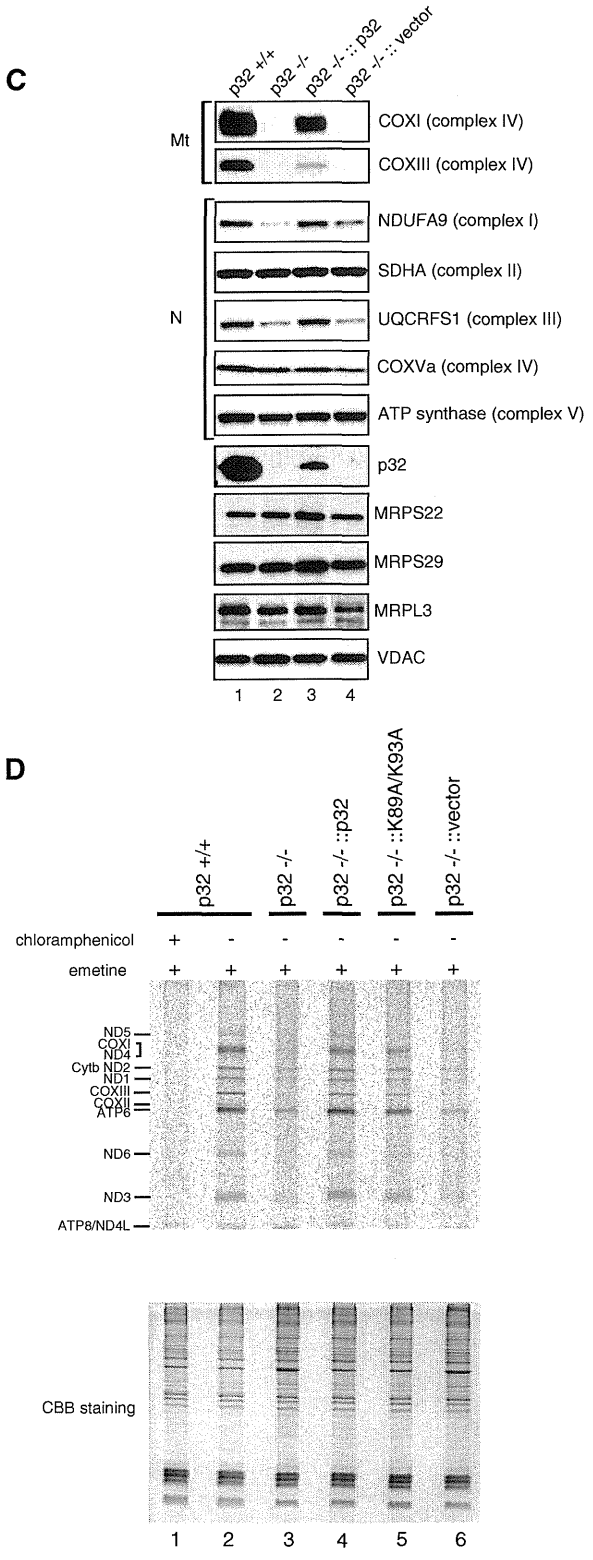

Figure 3. Continued.

respiratory chain by western blotting. Knockout of p32 resulted in a decrease in COXI and COXIII, subunit I and III of complex IV, which is encoded by mtDNA (Figure 3C). The loss of nuclear-encoded complex III subunit (UQCRFS1) may reflect the instability of the complex, which arises from general loss of mtDNA-encoded components, as shown later (Figure 3D). NDUFA9 (complex I) was slightly decreased in knockout cells. ATP synthase (complex V) barely changed. Re-expression of p32 in p32-knockout MEFs ($p32^{-/-}$::*p32*) restored mtDNA-encoded COXI, COXIII and nuclear-encoded NDUFA9, and UQCRFS1, but introduction of the vector only ($p32^{-/-}$::vector) did not rescue the levels of these proteins. There were no differences in the expression level of the complex II 70-kDa subunit (SDHA) or in the levels of mitochondrial proteins VDAC, mitochondrial ribosomal protein (MRP) S29 and S22, again indicating that p32 knockout specifically affects the levels of complexes I, III and IV.

Reduced mitochondrial translation rate

Next, to investigate the defect in mitochondrial protein synthesis, wild-type and knockout MEFs were pulse-labeled with a mixture of [^{35}S]-methionine and [^{35}S]-cysteine. To distinguish between proteins synthesized in the cytoplasm and mitochondria, cells were pre-treated with emetine and/or chloramphenicol, which are specific inhibitors of cytoplasmic and mitochondrial protein synthesis, respectively. Electrophoresis of whole-protein extracts from emetine-treated cells showed radioactive bands in the control (Figure 3D, lane 2). This profile clearly showed the products of mitochondrial protein synthesis. The synthesis of these proteins was completely inhibited by chloramphenicol (lane 1), confirming mitochondrial protein synthesis. This mitochondrial protein synthesis was strikingly reduced in p32-deficient cells (lane 3). This reduced protein synthesis was not caused by a reduction of mitochondrial mass, because there were no differences in the levels of mitochondrial proteins VDAC, MRPS29 and MRPL3, as shown in Figure 3C, which indicated that the mitochondrial mass in p32-deficient cells was normal. Re-expression of p32 in p32-deficient MEFs partially recovered the translation (lane 4). These results suggest that p32 deficiency results in a defect of mitochondrial protein synthesis.

Depletion of p32 affects mitoribosome distribution

Protein synthesis within mitochondria is performed by 55S mitoribosomes, which consist of a small 28S subunit and a large 39S subunit. There were no differences in the levels of mitoribosomal proteins such as MRPS29, MRPS22 and MRPL3, indicating that the total quantity of mitoribosomal subunits in p32-deficient cells was not largely affected (Figure 3C). To clarify the role of p32 in mitochondrial translation, we analyzed sedimentation profiles in a sucrose density gradient (Figure 4A and Supplementary Figure S4). The small and large subunits were traced with antibodies against MRPS29 and MRPL3, respectively, and were compared between wild-type, p32-knockout and p32-re-expressed MEFs. Similar levels of the 28S small subunit (fractions 5–6) and 39S large subunit (fractions 7–8) were found in the MEFs of these three cell lines. The 55S mitoribosome was mainly distributed in fractions 9 and 10 observed as the second peaks in MRPS29 and MRPL3 plots (Figure 4B).

However, in $p32^{-/-}$ cells, 55S formation were decreased. In p32-re-expressed cells, 55S ribosome formation was slightly recovered (fractions 9–10). The mitoribosomes broadly spanning the heavier fractions (fractions 11–16) may have represented translating multi-mitoribosomes or aggregated form. After treatment with EDTA in wild-type p32 MEF cells, 55S mitoribosome and heavier ribosome (fractions 11–16) were decreased and resemble as the $p32^{-/-}$ cells pattern (Supplementary Figure S4). These results suggested that p32 deficiency barely affected mitoribosome biogenesis (monosome formation), but did affect the formation of functioning 55S mitoribosomes. Though p32 mainly existed in the lighter fractions 1–4, it was also found in fractions 5–16. Considering that p32 is an abundant and multi-associated protein, p32 may functionally interact with the mitoribosome, although it is not integrated into it. Taken together, we theorize that p32 depletion somehow affects the formation of a functioning mitoribosome.

p32 binds to mitochondrial mRNA

Protein–RNA interactions play essential roles in post-transcriptional control of gene expression, including in mRNA degradation and translational regulation. p32 was originally copurified with the pre-mRNA splicing factor SRSF1 from human HeLa cells (22). In addition, p32 was designated a mitochondrial RNA-binding protein by proteomic studies (18). These studies suggest an RNA-binding ability of p32. To test whether p32 was able to bind mitochondrial mRNA, hemagglutinin-tagged p32 (p32-HA) protein was expressed in HeLa cells and immunoprecipitated from total cell lysates. RNA was extracted from the immunoprecipitate (pellet). The p32-bound mRNAs were directly quantified by qRT–PCR and northern blotting (Figure 5 and Supplementary Figure S5). After induction of p32-HA, a substantial enrichment of the immunoprecipitate was observed for all 11 mitochondrial transcripts analyzed, but cytoplasmic mRNAs (*MAPK6* and *β-actin*) were not enriched (Figure 5A, left panel), confirming that p32 was able to interact with mitochondrial mRNA *in vivo*. After IP using the anti-p32 antibody and $p32^{+/+}$ MEFs, we also observed that mitochondrial mRNAs, including ND1 and ND3 mRNAs, were enriched (Figure 5A and B), suggesting that p32 was also bound to mitochondrial mRNA in mouse cells. Northern blotting showed that ND1 and

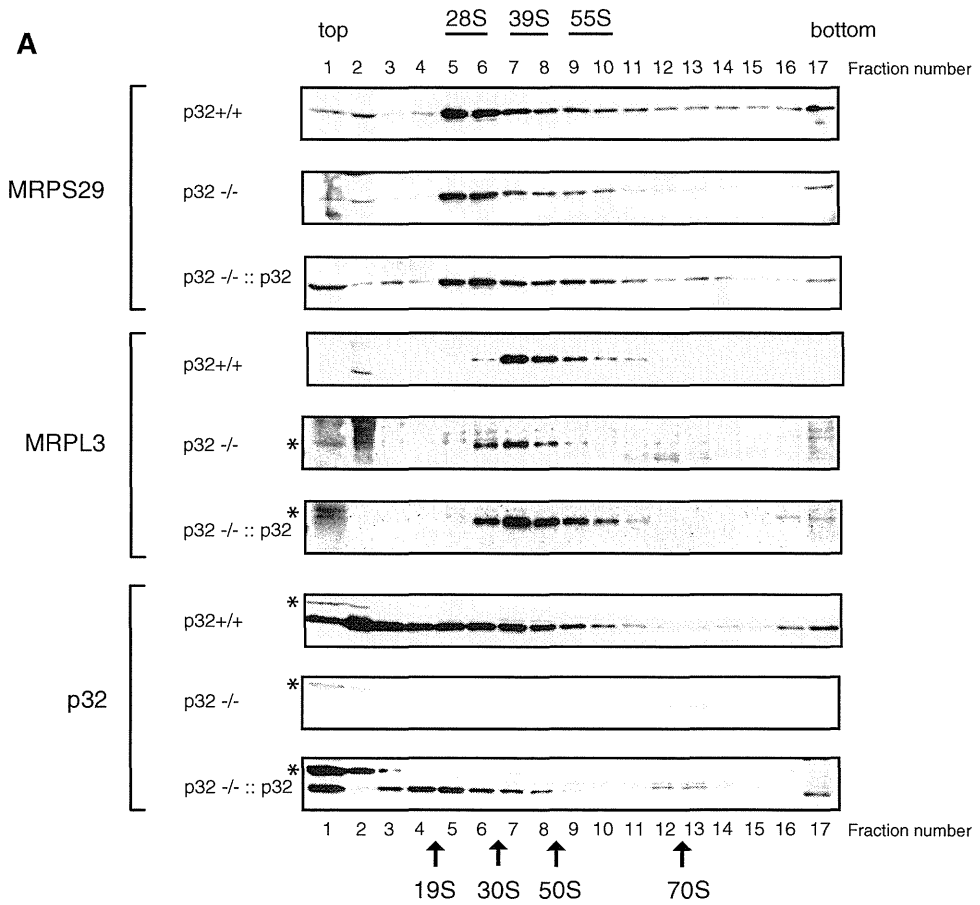

Figure 4. Reduction of p32 results in decreased mitoribosomes. (**A**) Upper panels: Sedimentation analysis of mitoribosomal particles by centrifugation via a linear 15–30% sucrose density gradient. Fraction numbers are indicated. The migration of mitoribosomal particles in wild-type (+/+), p32-knockout ($^{-/-}$) MEFs and p32 re-expressed ($^{-/-}$::p32) MEFs was determined by immunoblotting with antibodies against MRPL3 (39S large subunit), MRPS29 (28S small subunit) and p32. Arrows indicate peaks of optical density for the S value markers. Asterisk (*) shows non-specific band of MRPL3 and p32 at top fraction (1–2). (**B**) Representative blots were analyzed densitometrically. The signal intensity of the protein in each fraction was plotted. The maximum value was 100% for each protein level.

(continued)

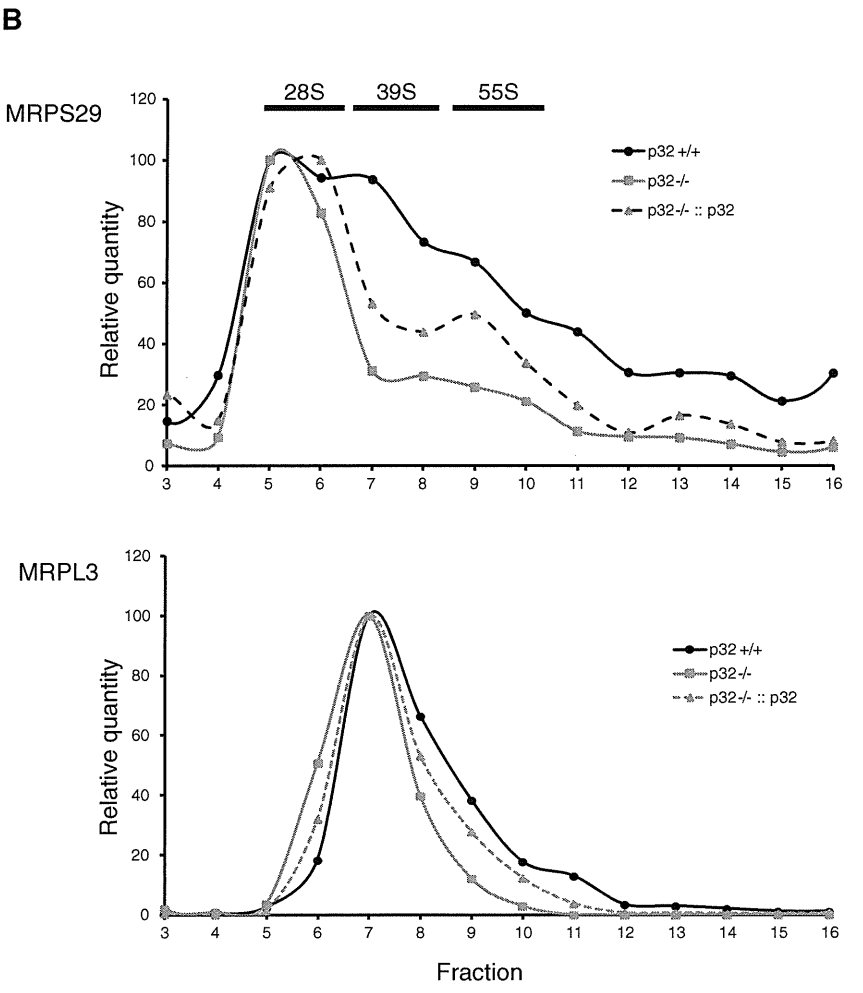

Figure 4. Continued.

COX1 mRNAs were detected at the same size after IP of p32, but cytoplasmic *β-actin* mRNA were not detected, which suggests that p32 was bound to these intact mitochondrial mRNAs (Figure 5C). We observed that the LRPPRC which RNA binding to mtRNA were reported (45), was not bound to mitochondrial mRNA in this experimental condition (Figure 5A, right panel) or TFAM which bind to mtDNA was also not bound (data not shown). Enrichment of *12S* and *16S* rRNAs was also observed (Figure 5A). There are no mtDNA in IP sample, because of no detection of PCR product without reverse transcriptase treatment (data not shown). 12S and 16S rRNAs were likely to be enriched via ribosome binding because western blotting of the eluates from the IPs showed that large and small mitoribosomal subunit proteins, MRPS22 and MRPL3, were co-immunoprecipitated with p32-HA (Figure 7). Taken together, these data are consistent with p32-association with all mitochondrial mRNAs in the mitochondrial matrix.

p32 binds to RNA oligonucleotides *in vitro*

Because p32 deficiency did not reduce mtDNA transcripts or affect biogenesis of mitoribosomes (Figures 3C and 4A), and p32 interacted with all mitochondrial mRNAs (Figure 5A and Figure 5B), we considered that p32 may bind to mRNAs via their poly(A) tail or in a sequence-independent manner. To test this hypothesis, we investigated the interaction of recombinant p32 protein with several RNA oligonucleotides *in vitro*. A REMSA showed that recombinant p32 protein clearly bound to a 22-mer poly(A) RNA in a dose-dependent manner (Figure 6A, lanes 1–7), while control glutathione-*S*-transferase (GST) protein and recombinant histidine (His)-tagged TFAM protein did not, indicating that this interaction was not mediated by the GST- or His-tag (Figure 6A, lanes 14-19). An interaction was not observed with a single-stranded, 22-mer poly(A) DNA oligonucleotide (Figure 6B, lanes 13–15), indicating that the p32 interaction was RNA-specific. The interaction with the 22-mer poly(U) RNA oligonucleotide was very weak (lanes 7–9). We also observed that recombinant p32 protein clearly bound to random 14- and 40-mer RNAs in a dose-dependent manner (Figure 6B, lanes 19–21 and 25–27), indicating that the p32 interaction was not sequence-specific. Consistently, a competition assay showed that the retarded band was more strongly competed with by

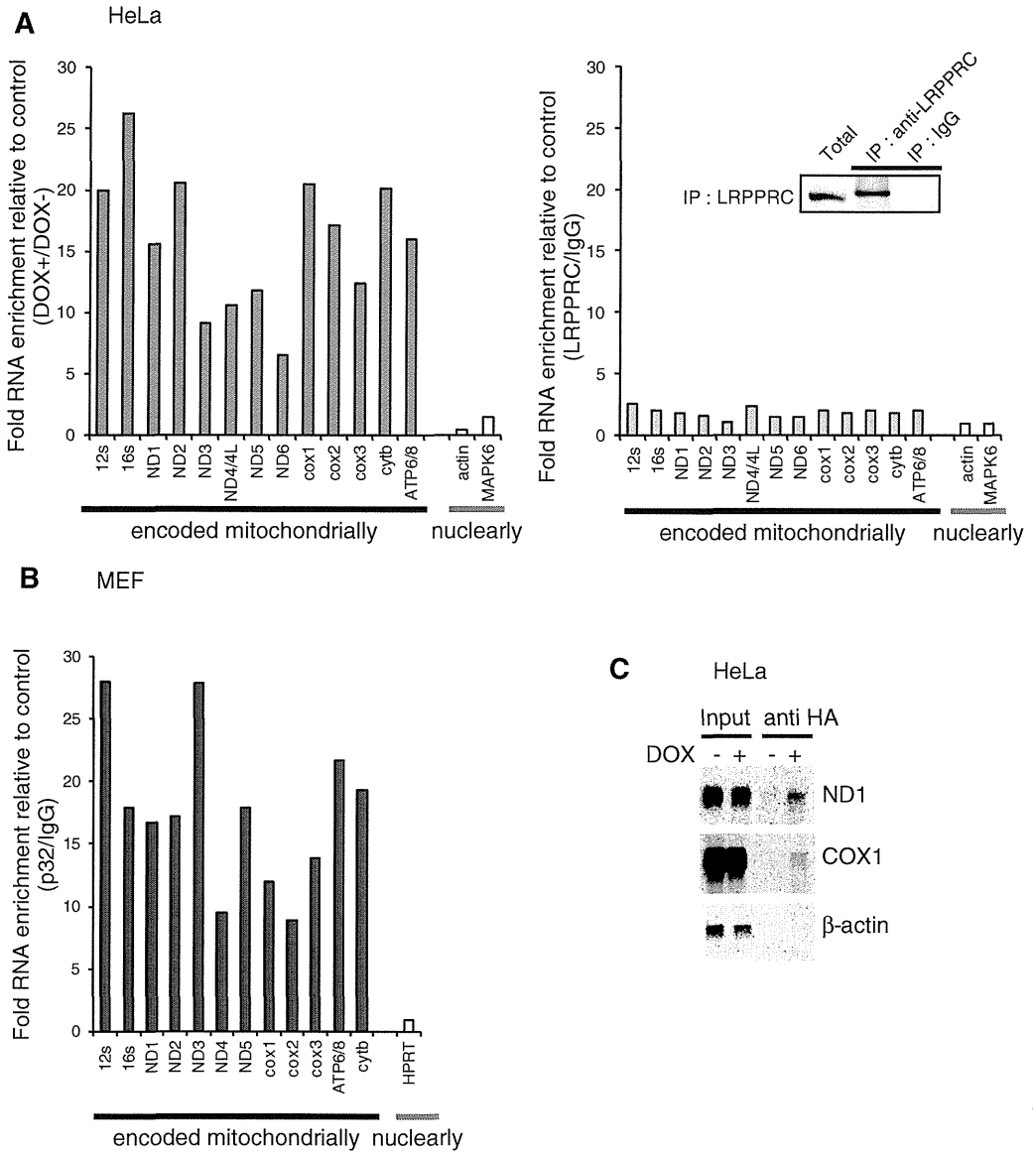

Figure 5. p32 interaction with RNA and the mitoribosome. (**A**) p32 is associated with mitochondrial RNA in HeLa cells. p32-HA expression in HeLa cells was induced with doxycycline (DOX+) or not (DOX–). HA-tagged p32 was immunoprecipitated (left panel). LRPPRC was also immunoprecipitated using the LRPPRC antibody and confirmed the IP by western blotting (right panel). The each RNA levels were measure by qPCR and the ratio of each RNA level (LRPPRC/IgG) is shown for mitochondria- and nuclear-encoded genes. (**B**) In MEF cells, p32 were immunoprecipitated using the p32 antibody. Then RNA was extracted from the immunoprecipitated samples and each RNA species was measured by qPCR as described in the materials and methods. The ratio of each RNA level (p32/ IgG) is shown for mitochondria- and nuclear-encoded genes. (**C**) Co-IP of RNA visualized on northern blot analysis in HeLa cells. RNA from whole-cell lysates (lanes 1 and 2) and immunoprecipitants with anti-HA (lanes 3 and 4) were loaded on gels. Northern blot analysis was performed using ND1, COX1 and β-actin probes.

unlabeled 40-mer RNA than by 22-mer poly(A) RNA and 14-mer RNA (Figure 6C), indicating that p32 bound to RNA with a length dependency. The retarded band was not competed with by unlabeled poly(A) DNA (Figure 6C). These results suggest that p32 binds to mitochondrial mRNAs in a manner dependent on length, but not sequence.

Lysine acetylation is a reversible post-translational protein modification. In many proteins, the acetylation plays a key role in regulating gene expression and protein function. A global analysis of lysine acetylation revealed that lysines 91 and 95 of human p32 were acetylated (46). These basic amino acid residues in the α helix H1, which is located on the edge of p32, may be able to provide electrostatic interactions with the RNA phosphate groups, raising a possibility of the involvement of the two lysines in the RNA binding. Therefore, we focused on the corresponding lysines in mouse p32, i.e. helix 1 K89 and K93 (Figure 6A, lanes 8–13). We constructed a double mutant, K89A/K93A, in which the two lysine residues were replaced by alanine. The RNA-binding activities of His-fusion wild-type and mutant p32 proteins to 22-mer poly(A) RNA, random 14-mer and random 40-mer RNAs were analyzed by a REMSA (Figure 6B, lanes 4–6, 10–12,

22–24 and 28–30). Mutant p32 showed a very weak RNA–protein complex band. The dissociation constant (K_d) of the complex for wild-type p32 was estimated to be 6 μM by a mobility-shift assay. However, the p32 lysine mutant diminished poly(A) affinity up to K_d 20 μM (Figure 6A). This mutant p32 retained the same intact trimer structure as wild-type p32 as revealed by size exclusion chromatography (Supplementary Figure S6). These results suggest that the lysine residues in α helix H1 are involved in this RNA binding.

To examine the importance of the RNA-binding activity of p32 in mitochondrial translation, we re-expressed

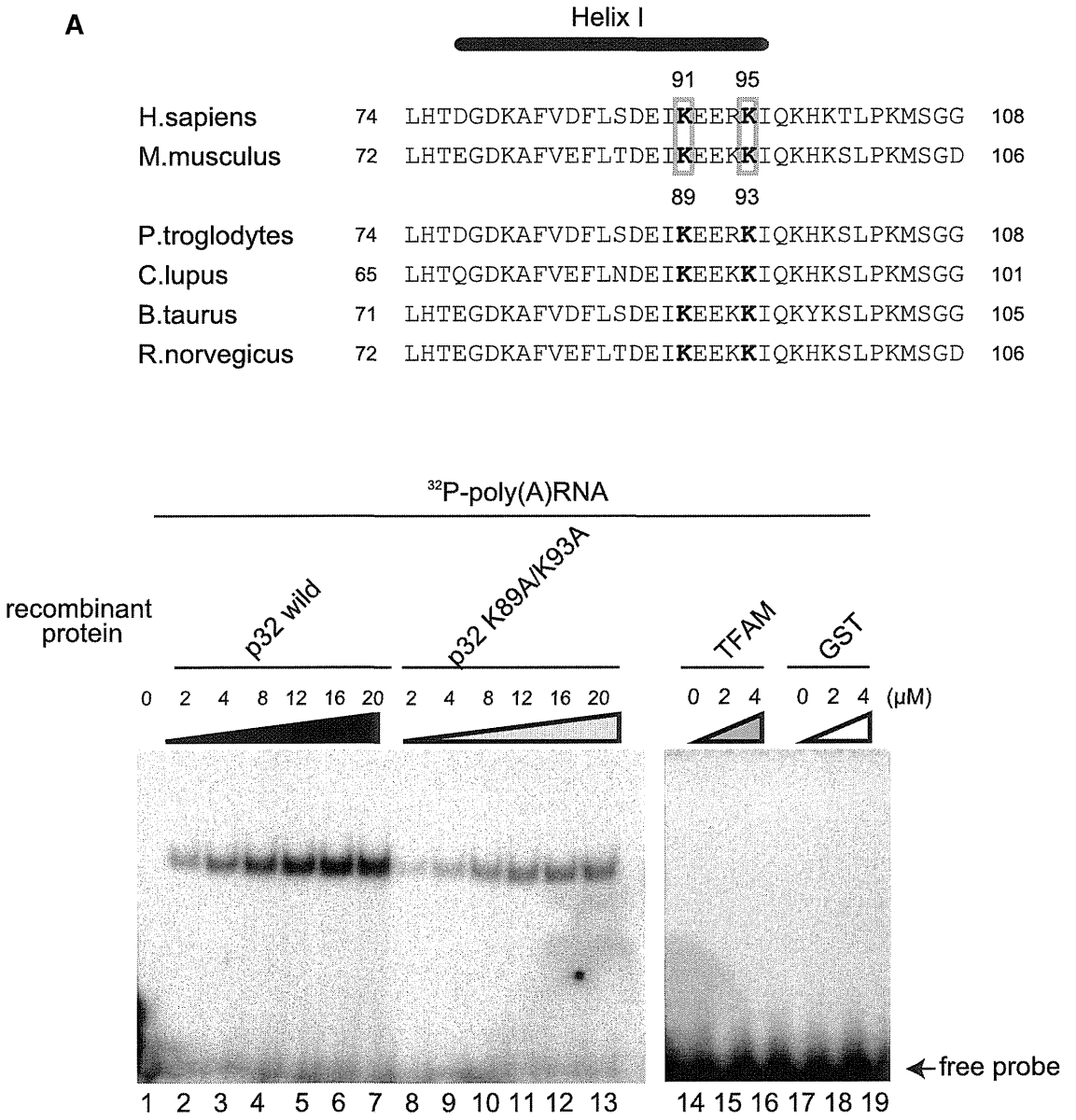

Figure 6. p32 binds to RNA oligonucleotides *in vitro*. (**A**) Upper: diagram of alignment in the α helix I of *Homo sapiens*, *Mus musculus*, *Pan troglodytes*, *Canis lupus*, *Bos taurus* and *Rattus norvegicus* p32. K89 and K93 in mouse p32 are shown as bold. Lower: purified wild-type and mutant p32, but not recombinant TFAM-His and GST proteins, bind to poly(A) oligonucleoside. Protein–poly(A) RNA complexes were separated by a REMSA using a 6% native polyacrylamide gel. An arrow indicates free probe. Recombinant wild-type and mutant proteins (2–20 μM) were incubated with 22-mer poly(A) RNA and then separated by a REMSA. Purified p32 bind to poly(A) oligonucleotide prefer to mutant p32. (**B**) The indicated amount of wild-type His-p32 and mutant His-p32 (K89A/K93A) fusion protein was incubated with ^{32}P-labeled random 14-mer RNA, 40-mer RNA, 22-mer poly(A) RNA, 22-mer poly(U) RNA or 22-mer poly(A) DNA oligonucleotides at 25°C for 30 min. p32–oligonucleotide complexes were separated by a electrophoretic REMSA using a 6% native polyacrylamide gel. The arrow indicates free probe. (**C**) Competition assays were performed by adding unlabeled RNA or DNA. The indicated fold amount of unlabeled RNA or DNA (0.2×, 1.0× or 5.0× relative to the ^{32}P-labeled probe) was incubated with recombinant p32 (4 μM) and ^{32}P-labeled poly(A) RNA; the complexes were separated by native polyacrylamide gel electrophoresis. The arrow indicates free probe. The lower panel indicates the intensity of the complex band. The 100% value represents the intensity of the complex of recombinant p32 and ^{32}P-labeled poly(A) RNA. (**D**) Expression of mitochondrial proteins. Cell lysates were prepared from equal amounts of wild-type MEFs, p32-knockout MEFs and MEFs with reintroduced wild-type *p32* cDNA, vector-only cDNA and mutant K89A/K93A *p32* cDNA. Blots were incubated with antibodies for the indicated proteins.

(continued)

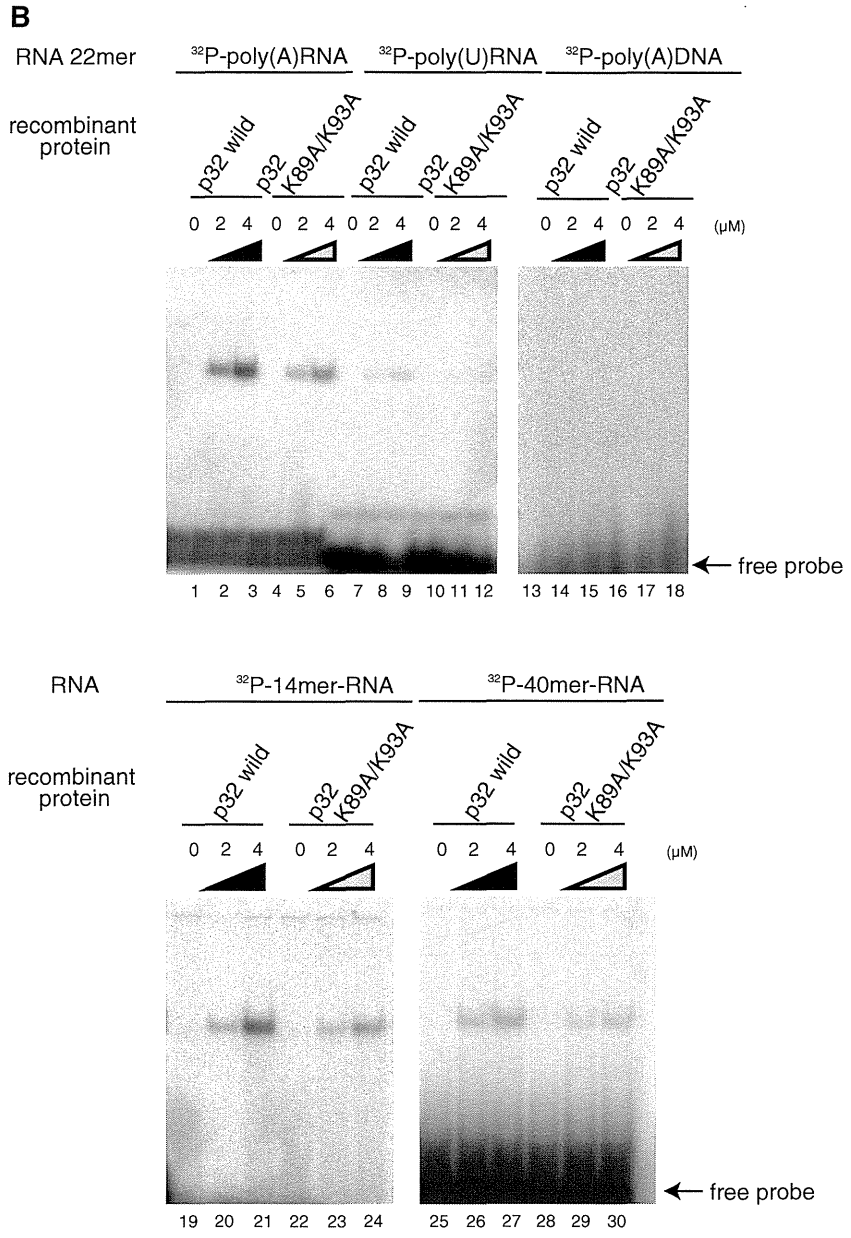

Figure 6. Continued.

wild-type and K89A/K93A mutant p32 in p32-knockout MEFs. The two p32 proteins were expressed to a similar degree (Figure 6D, lanes 3 and 5 in the uppermost panel). p32 deficiency caused defects of mitochondrial COXI and COXIII (lanes 1 and 2). Re-expression of wild-type p32 restored COXI and COXIII (lane 3). However, re-expression of the lysine mutant p32 restored COXI and COXIII much more weakly than did the wild-type p32 (lane 5). There were no differences in the expression levels of SDHA and β-actin, indicating that the lysine residues of p32 partially affected the COXI and COXIII protein level. We also performed *in vivo* labeling using the K89A/K93A mutant and observed that translation synthesis of the p32 mutant was less than the re-expressed wild-type p32 (Figure 3D, lanes 4 and 5). The COXI restoration ability of the K89A/K93A mutant was well correlated with its RNA-binding ability (Figure 6A and D). These results suggest that the RNA-binding ability of p32 is important for mitochondrial protein synthesis in mammalian cells.

Proteins associated with human p32

To further examine the association of p32 with translating mitoribosomes, we sought proteins that interacted with p32 in mitochondria. We immunoprecipitated p32-HA-associated proteins with anti-HA antibodies after cross-linking reactions in HeLa cells (Supplementary Figure S7). The cross-linked proteins that were identified by LC–MS/MS are listed in Table 2. This analysis revealed many mitoribosomal proteins, supporting the

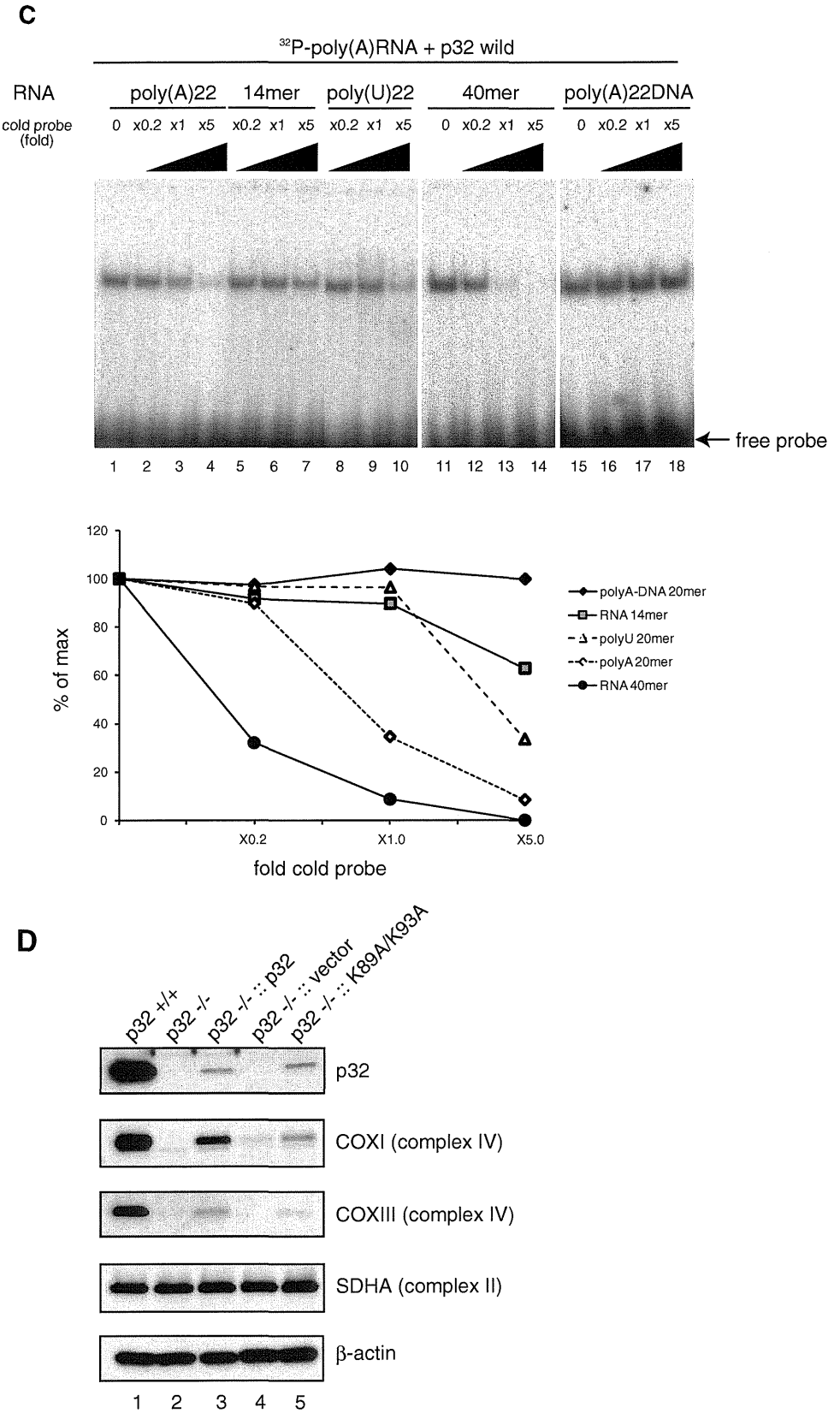

Figure 6. Continued.

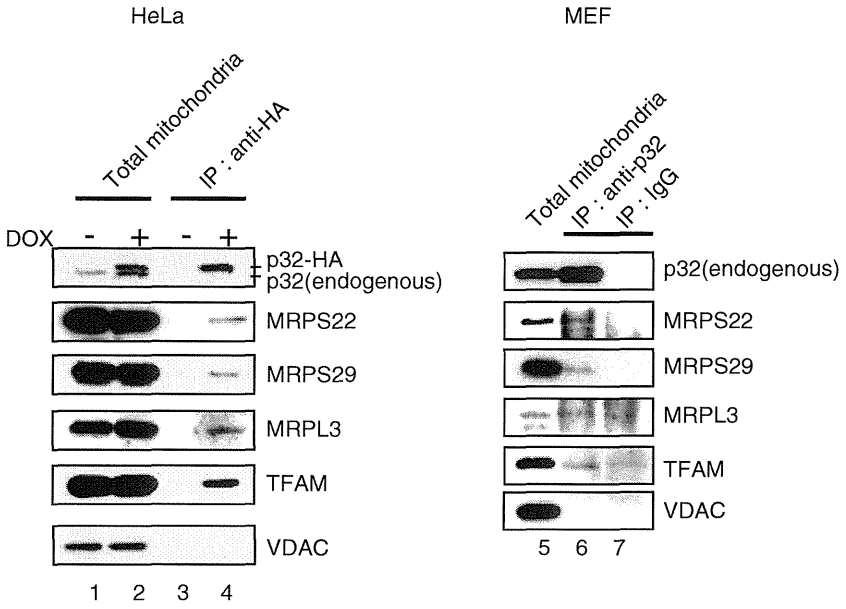

Figure 7. p32 interact with several ribosomal protein. p32-HA expression in HeLa cells was induced with doxycycline (DOX+) or not (DOX–). Lysed mitochondria were immunoprecipitated with anti-HA agarose (left panel), and a lysate of $p32^{+/+}$ MEFs was immunoprecipitated with an anti-p32 antibody (right panel) followed by western blotting with antibodies for the indicated proteins.

Table 2. List of proteins identified in complex with p32

Function	Gene				
28S ribosomal	MRPS10	MRPS2	MRPS22	MRPS23	MRPS25
	MRPS26	MRPS27	MRPS28	DAP3	MRPS30
	MRPS34	MRPS5	MRPS9	MRPS7	
39S ribosomal	MRPL12	MRPL18	MRPL19	MRPL21	MRPL22
	MRPL38	MRPL4	MRPL44	MRPL45	MRPL46
Chaperone	HSPD1	HSPA9	HSPA8	TRAP1	
Translation	ERAL1	TSFM	TUFM		
RNA binding	LRPPRC	PTCD3			
Protease	LONP1	CLPX			
Transcription	TFB2M	TFAM			
Others	PHB	PHB2			

role of p32 in the translation. In addition, many proteins that were related to nucleoids, RNA-binding and translation machinery were identified by LC-MS/MS. To confirm the association of p32 with ribosomal proteins, we carried out IP and western blotting using p32-HA-overexpressing HeLa cells and $p32^{+/+}$ MEFs. Ribosomal proteins including MRPS22, MRPS29 and MRPL3 were detected in the immunoprecipitates. However, VDAC were not immunoprecipitated with anti-p32 antibodies (Figure 7). These results suggest that p32 is associated with mitoribosomes in conjunction with all mitochondrial mRNAs for mitochondrial protein synthesis.

DISCUSSION

We have shown that p32 is essential for mouse embryonic development, based on the following evidence: (i) p32 is ubiquitously expressed in whole-mouse embryonic tissue; (ii) embryos lacking p32 are shrunken, show significantly arrested development and die at approximately E10.5; (iii) mitochondria in p32-deficient MEFs show morphological aberrations, whereas other organelles appear to be unaffected. These results suggest that mitochondrial p32 is a key molecule in mouse embryonic development.

The function of p32 in mitochondria was investigated in knockout MEFs: $p32^{-/-}$ cells. The knockout cells show severely impaired activities of electron transfer chain complexes I, III and IV but not complex II, leading strong support to requirement of p32 for expression of the mitochondrial genome. We showed that p32 deficiency impairs protein synthesis, but does not cause loss of mtDNA and transcripts. We speculated that p32 can bind to mitochondrial mRNA, but p32 is not involved in stabilizing mitochondrial mRNA. There are many mitochondria RNA-binding protein such as PTCD1~4 and LRPPRC which might be involved in stabilizing the mt-mRNA, suggesting that loss of p32 protein have no effect on the steady-state levels of mRNAs. Thus, p32 appears to be specifically required for mitochondrial protein synthesis. In sucrose gradient centrifugation and western blot experiments, p32-knockout cells exhibited normal mitoribosomal subunit assembly, but decreased 55S mitoribosomes, suggesting that p32 is not required for the subunit assembly, but is required for correct functioning of mitoribosomes with mRNA. Co-IP assays showed that p32 interacts with all mitochondrially encoded mRNAs, at least in part via poly(A) binding, and localizes close to the mitoribosome.

In this study, we obtained stable $p32^{-/-}$ MEFs that expressed a low level of mitochondrially targeted p32 (Supplementary Figure S3). Even at low-level expression in $p32^{-/-}$ MEFs, re-expression of p32 in $p32^{-/-}$ cells partially restored complex activity, mitochondrial ATP production, cell proliferation and protein translation, suggesting that a small amount of p32 rescues the

mitochondrial respiratory function via mitochondrial translational regulation. We successfully expressed p32 protein with the same plasmid up to a similar level of endogenous p32 in a human cancer cell line (data not shown), suggesting that the mechanism of p32 expression in MEFs is different from that in human cancer cells.

The Shine-Dalgarno sequence in the 5′-untranslated region of prokaryotes and the 7-methylguanylate cap structure in eukaryotic cell cytoplasm facilitate ribosome binding and direct the ribosome to the start codon. In contrast, mitochondrial mRNAs do not possess 5′-untranslated nucleotides or a cap structure (13,47). The small subunit of mitoribosomes appears to tightly bind mitochondrial mRNA in a sequence-independent manner without initiation factors or an initiation tRNA(48). However, the exact mechanisms of mRNA binding to mitoribosomes are unclear. Because of the unusual characteristics of mitochondrial mRNAs, it is thought that the mRNA 'entry gate' on the small subunit recognizes the unique unstructured 5′-sequence of mitochondrial mRNA (49,50). Here, we observed that p32 is required for the association of mitochondrial mRNAs with mitoribosomes (Figures 5 and 7). One possible mechanism is that p32 mediates the binding of mRNA to the small subunit and consequently enhance 55S formation. In prokaryotes, it is believed that initiation of leaderless mRNA occurs in intact 70S ribosomes. In *p32*$^{-/-}$ cells, the 55S mitoribosome peak was strongly reduced (Figure 4B, upper panel). Hence, another possible mechanism is that p32 contributes to guiding this unique 5′-leaderless mRNA to mitoribosomes for initiation of translation in part by enhancing the mitoribosome formation or stabilizing the mitoribosome.

We observed that the total ATP level was significantly higher in p32-knockout MEFs than in wild-type MEFs (Figure 2D), and the total ATP level is almost the same as glycolytic ATP production in p32$^{-/-}$ MEFs. The knockdown of RelA, the dominant NF-κB transactivating subunit, markedly enhances glucose consumption and lactate production in MEFs under normal culture conditions. RelA-deficient cells also exhibit decreased oxygen consumption and cell survival, although they show increased ATP levels (51), the same as p32$^{-/-}$ MEFs, suggesting that p32- and RelA-deficient cells show increased ATP levels due to the high activity of aerobic glycolysis.

Using *in vivo* labeling, we showed that re-expression of p32 in p32-deficient MEFs partially recovers the translation (Figure 3D, lane 4). However, the ratio of each protein is almost the same as the wild-type (lane 2), indicating that mtDNA-encoded protein synthesis is equally and generally suppressed and restored in p32$^{-/-}$ cells and in p32-resotred cells, respectively. Re-introduction of p32 into p32$^{-/-}$ cells well rescues complex I activity, but cannot compensate the reduced activity of complexes III and IV to a similar extent. This discrepancy may be due to the number or function of the assembly factors of each complex.

Mitochondrial RNA-binding proteins identified in previous proteomic studies include mitochondrial ribosomal proteins, tRNA synthetases, AUH, p32, LRPPRC (leucine-rich PPR motif-containing protein) and ribonuclease H1. Ponamarev *et al.* performed a proteomic analysis of bovine mitochondrial proteins with affinity to polyadenylate or polyuridylate (18). Of the 64 identified proteins, 51 possess a defined mitochondrial function, including 6 known RNA-binding proteins such as AUH. That study also showed by affinity purification that mitochondrial adenylate kinase 3, AUH and carnitine acetyltransferase bound poly(A), but not poly(U), while p32 bound poly(U) but not poly(A). However, our *in vitro* cell-free experiments demonstrated that purified recombinant p32 preferentially binds poly(A) rather than poly(U) RNA. The reason for this discrepancy is currently unknown. p32 may bind poly(U) via another protein in a crude system.

Disruption of hyaluronan synthetase 2 gene by generation Has$^{-/-}$ transgenic mice also results in abnormalities during midgestation with severe cardiac and vascular deformities, having similar phenotypic changes that takes place with p32/gC1qR/HABP1-deficient mice (52). Apoptosis induction by mitochondrial accumulation of HABP1 in fibroblast cell line with the generation of ROS and inhibition in complex I and mitochondrial dysfunction is supporting the OXPHOS regulation of p32 (53).

Acetylation of lysine is a reversible post-translational modification, which neutralizes the positive charge of this amino acid and modulates protein function in diverse ways. It plays a key role in the regulation of gene expression via the modification of core histone tails by histone acetyltransferases and deacetylases. A global analysis of lysine acetylation showed that p32 is acetylated at lysines 91 and 95 in human cell lines (46), suggesting a possible role of the lysine acetylation in p32 function and mitochondrial mRNA regulation.

Three p32 molecules form a doughnut-shaped quaternary structure with a sizable central channel and an unusual asymmetric charge distribution on the surface. This structure is highly positively charged because of the Lys residues in the α helix H1, which are located at the edge of the cleft of p32. A row of Lys residues in the α helix H1 on the surface of the molecule is conserved between human and mouse p32. The distances between these Lys residues are similar to those between the RNA phosphate groups, raising the possibility that the lysine residues continuously bind to single-stranded RNA. The alanine mutation of the two lysines in fact decreased the RNA-binding activity of p32 (Figure 6). Combined with their structural position, the lysine pair in p32 could cooperatively contribute to binding a region of single-stranded RNA. These lysine residues are conserved only among the mammals (Figure 6A) and not conserved in *Caenorhabditis elegans* or *S. cerevisiae* (23). Hence, the two lysine residues K89/K93 of the mouse p32 might play an indirect or additional role in RNA binding and resultantly in mitochondrial translation. At present, it remains yet to be identified which amino acids of p32 directly bind to RNA. However, the present lysine mutation results clearly support the importance of RNA-binding ability of p32 for the mitochondrial translation.

Mammalian mitochondria contain their own genome that is almost fully transcribed from both strands, which generates polycistronic RNA units that are processed and

matured. Mitochondrial mRNAs are modified by oligo- or polyadenylation at their 3′-termini, but the exact function of this post-transcriptional addition is unclear. The role of polyadenylation in transcription may involve mRNA stability (54). To analyze the function of polyadenylation in mitochondria, Wydro *et al.* manipulated the mitochondrial mRNA poly(A) tail by targeting a cytosolic poly(A)-modifying enzyme (PABP1) to mitochondria. The observed decline in mitochondrial translation is likely due to a dominant negative action of mtPABP1 via disruption of essential protein–protein interactions in the poly(A) extension. These results indicate that poly(A) normally interacts with endogenous components that promote translation. However, coating of the poly(A) tail by mtPABP1 did not lead to transcript decay, but caused a marked inhibition of mitochondrial translation. It was also shown that removal of the 3′-adenylyl extensions results in a variable effect on mRNA steady-state levels, increasing ND1, ND2 and ND6 mRNAs or decreasing COX1 and COX2, which suggests that the mitochondrial RNA degradosome is involved in these changes. Those data are consistent with endogenous RNA-binding factor(s) such as p32 interacting with poly(A) to optimize mitochondrial protein synthesis and increase mRNA.

p32 is a very acidic protein with a calculated isoelectric point of 4 (23). In contrast, the one side of the doughnut-shape is much less negatively charged. This polarity in charge distribution clearly suggests asymmetric functional roles for the two sides of the protein. These conserved surface features are very likely to be important for protein–protein interactions and ligand binding. We observed that various proteins, such as mitoribosomal proteins, are associated with p32. In *Escherichia coli*, the majority of ribosomal proteins in both 30S and 50S subunits are basic. The acidic side of p32 may be involved in protein–protein interactions, such as those with the mitoribosome, while the other side of p32 is involved in binding RNA via its α helix H1.

RNA chaperones are proteins that non-specifically interact with RNA and promote RNA folding by either resolving non-native conformations or impeding their formation (55). Based on our findings that p32 shows significant RNA binding and stimulates translation, we speculate that RNA chaperoning is a major activity of p32. We suggest that the putative RNA chaperone activity of p32 contributes to RNA rearrangement during the early phase of translation initiation. A chaperoning function may be important for p32 to transport RNAs to the mitoribosome.

The RNA-binding ability is well correlated with the mitochondrial protein restoration ability in $p32^{-/-}$ MEFs. Thus, the RNA-binding activity of p32 may be critically important for proper and efficient translation in the mitochondrial matrix. p32 may not only guide mRNA to the mitoribosomes, but also markedly contribute to efficient initiation and/or elongation reactions, because mitoribosomes in the heavier fractions strongly decreased in $p32^{-/-}$ MEFs. Taken together, we provide the first demonstration that p32 plays a vital role in mitochondrial homeostasis and fetal development.

SUPPLEMENTARY DATA

Supplementary Data are available at NAR Online: Supplementary Table 1, Supplementary Figures 1–7 and Supplementary Methods.

ACKNOWLEDGEMENTS

The authors would like to acknowledge the technical expertise of the Support Center for Education and Research, Kyushu University, and Masami Takade for electron microscopy.

FUNDING

Grants-in-Aid for Scientific Research from the Ministry of Education, Science, Technology, Sports, and Culture of Japan (MEXT) [#19209019 and #21590337]. Funding for open access charge: MEXT.

Conflict of interest statement. None declared.

REFERENCES

1. Anderson,S., Bankier,A.T., Barrell,B.G., de Bruijn,M.H., Coulson,A.R., Drouin,J., Eperon,I.C., Nierlich,D.P., Roe,B.A., Sanger,F. *et al.* (1981) Sequence and organization of the human mitochondrial genome. *Nature*, **290**, 457–465.
2. Kang,D. and Hamasaki,N. (2005) Mitochondrial transcription factor A in the maintenance of mitochondrial DNA: overview of its multiple roles. *Ann. N Y Acad. Sci.*, **1042**, 101–108.
3. Asin-Cayuela,J. and Gustafsson,C.M. (2007) Mitochondrial transcription and its regulation in mammalian cells. *Trends Biochem. Sci.*, **32**, 111–117.
4. Rorbach,J., Soleimanpour-Lichaei,R., Lightowlers,R.N. and Chrzanowska-Lightowlers,Z.M. (2007) How do mammalian mitochondria synthesize proteins? Biochem. *Soc. Trans.*, **35**, 1290–1291.
5. Chen,X.J. and Butow,R.A. (2005) The organization and inheritance of the mitochondrial genome. *Nat. Rev. Genet.*, **6**, 815–825.
6. Kucej,M. and Butow,R.A. (2007) Evolutionary tinkering with mitochondrial nucleoids. *Trends Cell. Biol.*, **17**, 586–592.
7. Parisi,M.A. and Clayton,D.A. (1991) Similarity of human mitochondrial transcription factor 1 to high mobility group proteins. *Science*, **252**, 965–969.
8. Ohno,T., Umeda,S., Hamasaki,N. and Kang,D. (2000) Binding of human mitochondrial transcription factor A, an HMG box protein, to a four-way DNA junction. *Biochem. Biophys. Res. Commun.*, **271**, 492–498.
9. Shadel,G.S. (2008) Expression and maintenance of mitochondrial DNA: new insights into human disease pathology. *Am. J. Pathol.*, **172**, 1445–1456.
10. Kanki,T., Ohgaki,K., Gaspari,M., Gustafsson,C.M., Fukuoh,A., Sasaki,N., Hamasaki,N. and Kang,D. (2004) Architectural role of mitochondrial transcription factor A in maintenance of human mitochondrial DNA. *Mol. Cell. Biol.*, **24**, 9823–9834.
11. Clayton,D.A. (1991) Replication and transcription of vertebrate mitochondrial DNA. *Annu. Rev. Cell. Biol.*, **7**, 453–478.
12. Ojala,D., Montoya,J. and Attardi,G. (1981) tRNA punctuation model of RNA processing in human mitochondria. *Nature*, **290**, 470–474.
13. Montoya,J., Ojala,D. and Attardi,G. (1981) Distinctive features of the 5'-terminal sequences of the human mitochondrial mRNAs. *Nature*, **290**, 465–470.
14. Montoya,J., Lopez-Perez,M.J. and Ruiz-Pesini,E. (2006) Mitochondrial DNA transcription and diseases: past, present and future. *Biochim. Biophys. Acta*, **1757**, 1179–1189.

15. Tomecki,R., Dmochowska,A., Gewartowski,K., Dziembowski,A. and Stepien,P.P. (2004) Identification of a novel human nuclear-encoded mitochondrial poly(A) polymerase. *Nucleic Acids Res.*, **32**, 6001–6014.
16. Nagaike,T., Suzuki,T., Katoh,T. and Ueda,T. (2005) Human mitochondrial mRNAs are stabilized with polyadenylation regulated by mitochondria-specific poly(A) polymerase and polynucleotide phosphorylase. *J. Biol. Chem.*, **280**, 19721–19727.
17. Nakagawa,J., Waldner,H., Meyer-Monard,S., Hofsteenge,J., Jeno,P. and Moroni,C. (1995) AUH, a gene encoding an AU-specific RNA binding protein with intrinsic enoyl-CoA hydratase activity. *Proc. Natl Acad. Sci. USA*, **92**, 20512055.
18. Ponamarev,M.V., She,Y.M., Zhang,L. and Robinson,B.H. (2005) Proteomics of bovine mitochondrial RNA-binding proteins: HES1/KNP-I is a new mitochondrial resident protein. *J. Proteome Res.*, **4**, 43–52.
19. Lukong,K.E., Chang,K.W., Khandjian,E.W. and Richard,S. (2008) RNA-binding proteins in human genetic disease. *Trends Genet.*, **24**, 416–425.
20. Kurimoto,K., Fukai,S., Nureki,O., Muto,Y. and Yokoyama,S. (2001) Crystal structure of human AUH protein, a single-stranded RNA binding homolog of enoyl-CoA hydratase. *Structure*, **9**, 1253–1263.
21. Kurimoto,K., Kuwasako,K., Sandercock,A.M., Unzai,S., Robinson,C.V., Muto,Y. and Yokoyama,S. (2009) AU-rich RNA-binding induces changes in the quaternary structure of AUH. *Proteins*, **75**, 360–372.
22. Petersen-Mahrt,S.K., Estmer,C., Ohrmalm,C., Matthews,D.A., Russell,W.C. and Akusjarvi,G. (1999) The splicing factor-associated protein, p32, regulates RNA splicing by inhibiting ASF/SF2 RNA binding and phosphorylation. *EMBO J.*, **18**, 1014–1024.
23. Jiang,J., Zhang,Y., Krainer,A.R. and Xu,R.M. (1999) Crystal structure of human p32, a doughnut-shaped acidic mitochondrial matrix protein. *Proc. Natl Acad. Sci. USA*, **96**, 3572–3577.
24. Matthews,D.A. and Russell,W.C. (1998) Adenovirus core protein V interacts with p32–a protein which is associated with both the mitochondria and the nucleus. *J. Gen. Virol*, **79(Pt 7)**, 1677–1685.
25. van Leeuwen,H.C. and O'Hare,P. (2001) Retargeting of the mitochondrial protein p32/gC1Qr to a cytoplasmic compartment and the cell surface. *J. Cell Sci.*, **114**, 2115–2123.
26. Soltys,B.J., Kang,D. and Gupta,R.S. (2000) Localization of P32 protein (gC1q-R) in mitochondria and at specific extramitochondrial locations in normal tissues. *Histochem. Cell. Biol.*, **114**, 245–255.
27. Muta,T., Kang,D., Kitajima,S., Fujiwara,T. and Hamasaki,N. (1997) p32 protein, a splicing factor 2-associated protein, is localized in mitochondrial matrix and is functionally important in maintaining oxidative phosphorylation. *J. Biol. Chem.*, **272**, 24363–24370.
28. Bharadwaj,A., Ghosh,I., Sengupta,A., Cooper,T.G., Weinbauer,G.F., Brinkworth,M.H., Nieschlag,E. and Datta,K. (2002) Stage-specific expression of proprotein form of hyaluronan binding protein 1 (HABP1) during spermatogenesis in rat. *Mol. Reprod. Dev.*, **62**, 223–232.
29. Rubinstein,D.B., Stortchevoi,A., Boosalis,M., Ashfaq,R., Ghebrehiwet,B., Peerschke,E.I., Calvo,F. and Guillaume,T. (2004) Receptor for the globular heads of C1q (gC1q-R, p33, hyaluronan-binding protein) is preferentially expressed by adenocarcinoma cells. *Int. J. Cancer*, **110**, 741–750.
30. Sunayama,J., Ando,Y., Itoh,N., Tomiyama,A., Sakurada,K., Sugiyama,A., Kang,D., Tashiro,F., Gotoh,Y., Kuchino,Y. *et al.* (2004) Physical and functional interaction between BH3-only protein Hrk and mitochondrial pore-forming protein p32. *Cell Death Differ.*, **11**, 771–781.
31. Itahana,K. and Zhang,Y. (2008) Mitochondrial p32 is a critical mediator of ARF-induced apoptosis. *Cancer Cell*, **13**, 542–553.
32. Storz,P., Hausser,A., Link,G., Dedio,J., Ghebrehiwet,B., Pfizenmaier,K. and Johannes,F.J. (2000) Protein kinase C [micro] is regulated by the multifunctional chaperon protein p32. *J. Biol. Chem.*, **275**, 24601–24607.
33. Jha,B.K., Salunke,D.M. and Datta,K. (2003) Structural flexibility of multifunctional HABP1 may be important for regulating its binding to different ligands. *J. Biol. Chem.*, **278**, 27464–27472.
34. Spicer,A.P. and Tien,J.Y. (2004) Hyaluronan and morphogenesis. *Birth Defects Res. C Embryo Today*, **72**, 89–108.
35. Mallick,J. and Datta,K. (2005) HABP1/p32/gC1qR induces aberrant growth and morphology in Schizosaccharomyces pombe through its N-terminal alpha helix. *Exp. Cell Res.*, **309**, 250–263.
36. Fogal,V., Richardson,A.D., Karmali,P.P., Scheffler,I.E., Smith,J.W. and Ruoslahti,E. (2010) Mitochondrial p32 protein is a critical regulator of tumor metabolism via maintenance of oxidative phosphorylation. *Mol. Cell. Biol.*, **30**, 1303–1318.
37. Uchiumi,T., Ohgaki,K., Yagi,M., Aoki,Y., Sakai,A., Matsumoto,S. and Kang,D. (2010) ERAL1 is associated with mitochondrial ribosome and elimination of ERAL1 leads to mitochondrial dysfunction and growth retardation. *Nucleic Acids Res.*, **38**, 5554–5568.
38. Claypool,S.M., Oktay,Y., Boontheung,P., Loo,J.A. and Koehler,C.M. (2008) Cardiolipin defines the interactome of the major ADP/ATP carrier protein of the mitochondrial inner membrane. *J. Cell Biol.*, **182**, 937–950.
39. Hofhaus,G., Shakeley,R.M. and Attardi,G. (1996) Use of polarography to detect respiration defects in cell cultures. *Methods Enzymol*, **264**, 476–483.
40. Estornell,E., Fato,R., Pallotti,F. and Lenaz,G. (1993) Assay conditions for the mitochondrial NADH:coenzyme Q oxidoreductase. *FEBS Lett.*, **332**, 127–131.
41. Trounce,I.A., Kim,Y.L., Jun,A.S. and Wallace,D.C. (1996) Assessment of mitochondrial oxidative phosphorylation in patient muscle biopsies, lymphoblasts, and transmitochondrial cell lines. *Methods Enzymol.*, **264**, 484–509.
42. Brautigan,D.L., Ferguson-Miller,S. and Margoliash,E. (1978) Mitochondrial cytochrome c: preparation and activity of native and chemically modified cytochromes c. *Methods Enzymol.*, **53**, 128–164.
43. Ishihara,N., Nomura,M., Jofuku,A., Kato,H., Suzuki,S.O., Masuda,K., Otera,H., Nakanishi,Y., Nonaka,I., Goto,Y. *et al.* (2009) Mitochondrial fission factor Drp1 is essential for embryonic development and synapse formation in mice. *Nat. Cell Biol.*, **11**, 958–966.
44. Alirol,E. and Martinou,J.C. (2006) Mitochondria and cancer: is there a morphological connection? *Oncogene*, **25**, 4706–4716.
45. Ruzzenente,B., Metodiev,M.D., Wredenberg,A., Bratic,A., Park,C.B., Camara,Y., Milenkovic,D., Zickermann,V., Wibom,R., Hultenby,K. *et al.* (2012) LRPPRC is necessary for polyadenylation and coordination of translation of mitochondrial mRNAs. *EMBO J.*, **31**, 443–456.
46. Choudhary,C., Kumar,C., Gnad,F., Nielsen,M.L., Rehman,M., Walther,T.C., Olsen,J.V. and Mann,M. (2009) Lysine acetylation targets protein complexes and co-regulates major cellular functions. *Science*, **325**, 834–840.
47. Grohmann,K., Amairic,F., Crews,S. and Attardi,G. (1978) Failure to detect "cap" structures in mitochondrial DNA-coded poly(A)-containing RNA from HeLa cells. *Nucleic Acids Res.*, **5**, 637–651.
48. Liao,H.X. and Spremulli,L.L. (1989) Interaction of bovine mitochondrial ribosomes with messenger RNA. *J. Biol. Chem.*, **264**, 7518–7522.
49. Sharma,M.R., Koc,E.C., Datta,P.P., Booth,T.M., Spremulli,L.L. and Agrawal,R.K. (2003) Structure of the mammalian mitochondrial ribosome reveals an expanded functional role for its component proteins. *Cell*, **115**, 97–108.
50. Jones,C.N., Wilkinson,K.A., Hung,K.T., Weeks,K.M. and Spremulli,L.L. (2008) Lack of secondary structure characterizes the 5' ends of mammalian mitochondrial mRNAs. *RNA*, **14**, 862–871.
51. Mauro,C., Leow,S.C., Anso,E., Rocha,S., Thotakura,A.K., Tornatore,L., Moretti,M., De Smaele,E., Beg,A.A., Tergaonkar,V. *et al.* (2011) NF-kappaB controls energy homeostasis and metabolic adaptation by upregulating mitochondrial respiration. *Nat. Cell Biol.*, **13**, 1272–1279.
52. Camenisch,T.D., Spicer,A.P., Brehm-Gibson,T., Biesterfeldt,J., Augustine,M.L., Calabro,A. Jr, Kubalak,S., Klewer,S.E. and

McDonald,J.A. (2000) Disruption of hyaluronan synthase-2 abrogates normal cardiac morphogenesis and hyaluronan-mediated transformation of epithelium to mesenchyme. *J. Clin. Invest.*, **106**, 349–360.
53. Chowdhury,A.R., Ghosh,I. and Datta,K. (2008) Excessive reactive oxygen species induces apoptosis in fibroblasts: role of mitochondrially accumulated hyaluronic acid binding protein 1 (HABP1/p32/gC1qR). *Exp. Cell Res.*, **314**, 651–667.
54. Wydro,M., Bobrowicz,A., Temperley,R.J., Lightowlers,R.N. and Chrzanowska-Lightowlers,Z.M. (2010) Targeting of the cytosolic poly(A) binding protein PABPC1 to mitochondria causes mitochondrial translation inhibition. *Nucleic Acids Res.*, **38**, 3732–3742.
55. Herschlag,D. (1995) RNA chaperones and the RNA folding problem. *J. Biol. Chem.*, **270**, 20871–20874.

BJ www.biochemj.org

Biochem. J. (2012) 443, 573–584 (Printed in Great Britain) doi:10.1042/BJ20111728

Ribonucleoprotein Y-box-binding protein-1 regulates mitochondrial oxidative phosphorylation (OXPHOS) protein expression after serum stimulation through binding to OXPHOS mRNA

Shinya MATSUMOTO, Takeshi UCHIUMI[1], Hiroyuki TANAMACHI, Toshiro SAITO, Mikako YAGI, Shinya TAKAZAKI, Tomotake KANKI and Dongchon KANG

Department of Clinical Chemistry and Laboratory Medicine, Graduate School of Medical Sciences, Kyushu University, 3-1-1 Maidashi, Higashi-ku, Fukuoka 812-8582, Japan

Mitochondria play key roles in essential cellular functions, such as energy production, metabolic pathways and aging. Growth factor-mediated expression of the mitochondrial OXPHOS (oxidative phosphorylation) complex proteins has been proposed to play a fundamental role in metabolic homoeostasis. Although protein translation is affected by general RNA-binding proteins, very little is known about the mechanism involved in mitochondrial OXPHOS protein translation. In the present study, serum stimulation induced nuclear-encoded OXPHOS protein expression, such as NDUFA9 [NADH dehydrogenase (ubiquinone) 1α subcomplex, 9, 39 kDa], NDUFB8 [NADH dehydrogenase (ubiquinone) 1β subcomplex, 8, 19 kDa], SDHB [succinate dehydrogenase complex, subunit B, iron sulfur (Ip)] and UQCRFS1 (ubiquinol-cytochrome *c* reductase, Rieske iron–sulfur polypeptide 1), and mitochondrial ATP production, in a translation-dependent manner. We also observed that the major ribonucleoprotein YB-1 (Y-box-binding protein-1) preferentially bound to these OXPHOS mRNAs and regulated the recruitment of mRNAs from inactive mRNPs (messenger ribonucleoprotein particles) to active polysomes. YB-1 depletion led to up-regulation of mitochondrial function through induction of OXPHOS protein translation from inactive mRNP release. In contrast, YB-1 overexpression suppressed the translation of these OXPHOS mRNAs through reduced polysome formation, suggesting that YB-1 regulated the translation of mitochondrial OXPHOS mRNAs through mRNA binding. Taken together, our findings suggest that YB-1 is a critical factor for translation that may control OXPHOS activity.

Key words: mitochondrion, messenger ribonucleoprotein particle (mRNP), oxidative phosphorylation (OXPHOS), translation, Y-box-binding protein-1 (YB-1).

INTRODUCTION

Mitochondria are essential organelles that are present in virtually all eukaryotic cells and have fundamental functions in energy production and other metabolic pathways. The primary function of mitochondria is ATP production via the OXPHOS (oxidative phosphorylation) pathway, which is subject to complex regulation, including short-term modulations that are essential for responding to transient changes in nutritional availability and energy requirements.

The mitochondrial genome does not possess a complete set of genes for assembly of the organelle. The circular 16.5 kb human mtDNA (mitochondrial DNA) molecule encodes two rRNAs, 22 tRNAs and 13 proteins that are members of the respiratory chain [1,2]. Most of the mitochondrial proteins are encoded in the nucleus and need to be imported into the organelle. After the proteins are fully synthesized in the cytosol, various assays have led to the widely accepted notion that import may occur post-translationally [3]. For the majority of the matrix proteins, mitochondrial transfer involves a specific N-terminal extension of the proteins that interacts with specific mitochondrial receptors [4]. Some of the cytosolic ribosomes were found to be bound to mitochondria [5], suggesting that these mitochondria-bound ribosomes are engaged in the synthesis of mitochondrial proteins and facilitate their transport into mitochondria, in accordance with a co-translational model [6].

The mitochondrial respiratory chain consists of five complexes, comprising more than 90 structural proteins [7]. Since only 13 proteins are encoded by mtDNA, almost 80 additional proteins are derived from the nuclear genome. Thus, to build the active OXPHOS complex, these additional proteins encoded by the nuclear genome are synthesized on cytosolic ribosomes, imported into the mitochondrial inner membrane and assembled with the mtDNA-encoded proteins.

Gene expression is regulated at both the transcriptional and translational levels in response to various conditions, but less is known about translational regulation compared with transcriptional regulation. A number of mRNA-binding proteins participate in translational regulation [8,9], and among these translational regulators, YB-1 (Y-box-binding protein-1) is a unique multifunctional protein that can regulate gene expression in both transcriptional and translational manners [10,11]. In both germinal and somatic cells, YB-1 is a major component of translationally inactive mRNPs (messenger ribonucleoprotein particles) and is mainly responsible for storage of mRNAs in a silent state.

Mammalian YB-1 is a member of the Y-box family proteins that contain a common structural feature, the cold shock domain, and control gene expression at the translational level through their

Abbreviations used: ActD, actinomycin D; ATP5A1, ATP synthase, H^+ transporting, mitochondrial F1 complex, α subunit 1, cardiac muscle; CHX, cycloheximide; 2-DG, 2-deoxy-D-glucose; eIF, eukaryotic initiation factor; FBS, fetal bovine serum; G3P, glycerol 3-phosphate; HA, haemagglutinin; IGF, insulin-like growth factor; mRNP, messenger ribonucleoprotein particle; mtDNA, mitochondrial DNA; NDUFA9, NADH dehydrogenase (ubiquinone) 1α subcomplex, 9, 39 kDa; NDUFB8, NADH dehydrogenase (ubiquinone) 1β subcomplex, 8, 19 kDa; OXPHOS, oxidative phosphorylation; P-body, processing body; PABP, poly(A)-binding protein; PI3K, phosphoinositide 3-kinase; qRT–PCR, quantitative reverse transcription–PCR; RT, reverse transcription; SDHA, succinate dehydrogenase complex, subunit A, flavoprotein (Fp); SDHB, succinate dehydrogenase complex, subunit B, iron sulfur (Ip); siRNA, small interfering RNA; TOR, target of rapamycin; UQCRFS1, ubiquinol-cytochrome *c* reductase, Rieske iron–sulfur polypeptide 1; YB-1, Y-box-binding protein-1.

[1] To whom correspondence should be addressed (email uchiumi@cclm.med.kyushu-u.ac.jp).

recognition of RNAs [10,12,13]. YB-1 associates with mRNA in polysomes or free mRNPs, depending on the molar ratio of YB-1 to its target mRNA, and functions as either an activator or inhibitor of translation [14,15]. Consistent with its essential biological functions, targeted disruption of YB-1 in mice causes severe developmental defects and embryonic lethality [16,17]. It has also been reported that YB-1 binds to the capped 5′-termini of mRNAs encoding proteins that are associated with cell growth and oncogenesis, and that Akt regulates this inhibitory effect on translation [18–20]. Specifically, Akt directly phosphorylates human YB-1 at Ser^{102}, which reduces the ability of YB-1 to bind to the cap of mRNAs and inhibit cap-dependent translation, and therefore induces the translation of silent mRNA species.

Protein synthesis is up-regulated in response to various signals, including growth factors, serum stimulation, hormones and cytokines, and is accompanied by the recruitment of translationally inactive mRNAs into polysomes [21]. The mitochondrial OXPHOS function is regulated by IGF (insulin-like growth factor) signalling, and up-regulation of respiration seems to require PI3K (phosphoinositide 3-kinase)/Akt signalling, suggesting that translational control is involved in this pathway and is implicated in controlling the rate of metabolism [22].

Therefore it is interesting to investigate the mechanism responsible for YB-1 after serum stimulation. First, we examined whether YB-1 similarly serves a mitochondrial OXPHOS function. It would be important to examine how YB-1 regulates translation in response to growth factors and how YB-1 depletion or overexpression regulated activation or inactivation of mRNA translation and maintained protein synthesis after serum-induced OXPHOS activity. These findings suggested that many of the YB-1-associated mRNAs encoded OXPHOS proteins, raising the possibility that serum-mediated YB-1 phosphorylation could, in part, increase the production of proteins regulating OXPHOS activity.

EXPERIMENTAL

Cell culture

Human cervical cancer HeLa cells were cultured in DMEM (Dulbecco's modified Eagle's medium) (Sigma) supplemented with 10 % (v/v) heat-inactivated FBS (fetal bovine serum; MP Biomedicals). The cells were incubated at 37 °C in a humidified atmosphere comprising 95 % air/5 % CO_2.

Immunoblot analysis

HeLa cells were lysed with TNE buffer (50 mM Tris/HCl, pH 7.5, 1 mM EDTA, 150 mM NaCl and 0.5 % Nonidet P40) and total lysates (10 μg) were subjected to immunoblot analysis as described previously [23] using polyclonal or monoclonal antibodies against YB-1 [17], NDUFA9 [NADH dehydrogenase (ubiquinone) 1α subcomplex, 9, 39 kDa], NDUFB8 [NADH dehydrogenase (ubiquinone) 1β subcomplex, 8, 19 kDa], SDHA [succinate dehydrogenase complex, subunit A, flavoprotein (Fp)], UQCRFS1 (ubiquinol-cytochrome *c* reductase, Rieske iron–sulfur polypeptide 1), ATP5A1 (ATP synthase, H^+ transporting, mitochondrial F1 complex, α subunit 1, cardiac muscle; Invitrogen), SDHB [succinate dehydrogenase complex, subunit B, iron sulfur (Ip)] (produced in our laboratory) and B23 (Santa Cruz Biotechnology). The signals were visualized with horseradish peroxidase-conjugated anti-rabbit or anti-mouse IgG and an enhanced chemiluminescence reagent (GE Healthcare). The chemiluminescence was recorded and quantified with a cooled charge-coupled device camera (LAS1000plus; FujiFilm).

Knockdown of YB-1 by siRNAs (small interfering RNAs)

The following double-stranded *YB-1* 25-bp RNA oligonucleotides were generated from Stealth Select RNAi (RNA interference; Invitrogen): 5′-UUUGCUGGUAAUUGCGUGGAGGACC-3′ and 5′-GGUCCUCCACGCAAUUACCAGCAAA-3′. siRNA transfections were performed according to the manufacturer's instructions (Invitrogen). Briefly, 2 μl of Oligofectamine™ (Invitrogen) was diluted in 50 μl of Opti-MEM I medium and incubated for 5 min at room temperature (25 °C). Next, 10 pmol of *YB-1* or control duplex Stealth RNA (Control siRNA; Invitrogen) in 50 μl of Opti-MEM I was added gently and incubated for 20 min at room temperature. Oligomer–Oligofectamine™ complexes and aliquots of 2×10^5 HeLa cells in 2 ml of culture medium were combined and incubated for 5 min at room temperature. The cells were seeded in six-well dishes with 2 ml of culture medium and subjected to a variety of analyses at 72 h.

Expression of YB-1 in HeLa Tet-on cells

A cDNA of *YB-1* was amplified from a human placenta cDNA library by PCR using the primer set 5′-CAGGATCCATGAG-CAGCGAGGCCGAGA-3′ and 5′-GAGCGGCCGCAACTCAG-CCCCGCCCTGCTCAG-3′, which added BamHI and NotI sites to the 5′ termini respectively. The PCR product was digested with BamHI and NotI. After a DNA fragment encoding an HA (haemagglutinin) tag and a pcDNA5/FRT/TO vector (Invitrogen) were digested with XhoI and ApaI and then ligated, the DNA fragment encoding YB-1 was ligated into the vector digested with BamHI and NotI. The resulting vector was designated pYB1-HA. We transfected HeLa/FRP/Tet-on cells with the pYB1-HA vector and selected cells bearing the transgene in the presence of hygromycin B (200 μg/ml) as described previously [24]. The expression of YB-1–HA was induced by doxycycline addition (100 μg/ml).

Immunoprecipitation using anti-HA antibodies

Immunoprecipitation was carried out using a previously described procedure [17]. Briefly, HeLa cell lysates induced by doxycycline were pre-cleared with recombinant Protein G–agarose (Invitrogen) for 30 min at 4 °C, followed by binding to anti-HA agarose beads (Sigma) for 2 h at 4 °C. The complexes were pulled down and washed five times with 1 ml of TNE buffer. The immunoprecipitated proteins were eluted with SDS sample buffer. RNA was extracted from the beads with an RNAeasy kit (Qiagen).

Quantification of RNA

Total RNA was extracted from HeLa cells and sucrose density gradient fractions using the RNAeasy kit. RT (reverse transcription) of 500 ng of the total RNA was performed with SuperScript III RT (Invitrogen) according to the manufacturer's instructions. The RT reaction mixtures were diluted 1:5 with water. The expression levels of nuclear-encoded mitochondrial genes were detected by quantitative PCR with a thermal cycler (StepOne plus, Invitrogen). The primer list is shown in Supplementary Table S1 (at http://www.BiochemJ.org/bj/443/bj4430573add.htm).

Sucrose gradient analysis

Cell lysates were prepared from HeLa cells treated with YB-1 or control siRNAs for 72 h, or YB-1–HA was induced by doxycycline. The HeLa cells were solubilized in a detergent solution (0.1 % SDS and 1.6 % Triton X-100). The post-nuclear

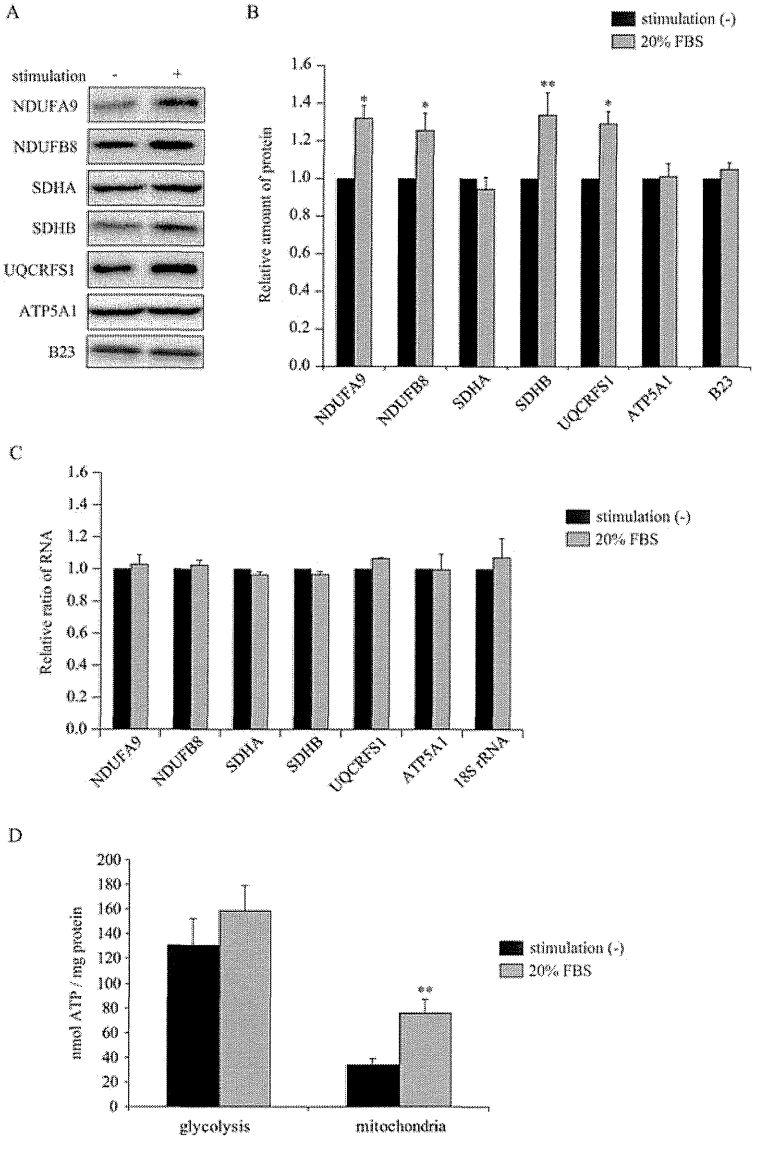

Figure 1 Nuclear-encoded OXPHOS proteins are up-regulated by serum stimulation

(**A**) HeLa cells were cultured for 21 h in serum-free medium and then stimulated with 20 % (v/v) FBS for 3 h. The cells were lysed and analysed by immunoblotting with antibodies against UQCRFS1, ATP5A1, NDUFB8, NDUFA9, SDHB and SDHA. (**B**) The intensities of the signals in (**A**) were analysed by densitometry. (**C**) HeLa cells were stimulated by 20 % (v/v) FBS for 3 h and RNA was extracted. The mRNA levels were analysed by qRT–PCR. (**D**) HeLa cells were treated with 20 mM 2-DG and 5 mM pyruvate for the last 5 h and stimulated with 20 % (v/v) FBS for the last 4 h. For the last 1 h, oligomycin was added to stop the mitochondrial ATP production. The cells were lysed and the ATP levels were measured using chemiluminescence and normalized with the amount of protein. Glycolytic ATP was calculated by subtracting the 2-DG-treated value from the untreated value, as total cellular ATP. Mitochondrial ATP was calculated by subtracting the 2-DG and oligomycin-treated value from the 2-DG-treated value. The results shown were obtained from three independent experiments and are means ± S.D. $^{*}P < 0.05$ and $^{**}P < 0.01$ by Student's t test.

supernatant was loaded on a 15–45 % (w/v) sucrose density gradient in 10 mM Tris/HCl, pH 7.2, containing 150 mM NaCl, and centrifuged at 33 000 rev./min for 3 h at 4 °C using a swinging bucket SW 41 Ti rotor (Beckman Coulter). After separation through the 15–45 % (w/v) sucrose gradient, the resulting fractions were precipitated with 10 % (v/v) trichloroacetic acid and washed in acetone, and the entire fractions were resolved by SDS/PAGE. For mRNA quantification, RNA was extracted from 40 μl aliquots of the fractions and assayed by qRT–PCR (quantitative RT–PCR).

ATP quantification

Cellular ATP was quantified using a CellTiter-Glo Luminescent Cell Viability Assay (Promega) according to the manufacturer's instructions. HeLa cells plated at equal densities were treated with 20 mM 2-DG (2-deoxy-D-glucose) and 5 mM pyruvate for 5 h. This allowed for inhibition of glycolysis while the cells were provided with the substrates necessary to generate ATP from mitochondrial metabolism. For the last 1 h, oligomycin was added to stop ATP production from complex V. The cells were lysed in passive lysis buffer (Promega) and evaluated using a chemiluminescence plate reader (ARVO 1420, Wallac). The values were normalized to the protein amounts in each lysate, and fell in the linear range of the assay as determined by a standard curve. Cellular ATP was assessed by splitting into glycolytic ATP and mitochondrial ATP. Glycolytic ATP was calculated by subtracting the 2-DG-treated value from the untreated value as total cellular ATP. Mitochondrial ATP was calculated by subtracting the 2-DG and oligomycin-treated value from the 2-DG-treated value.

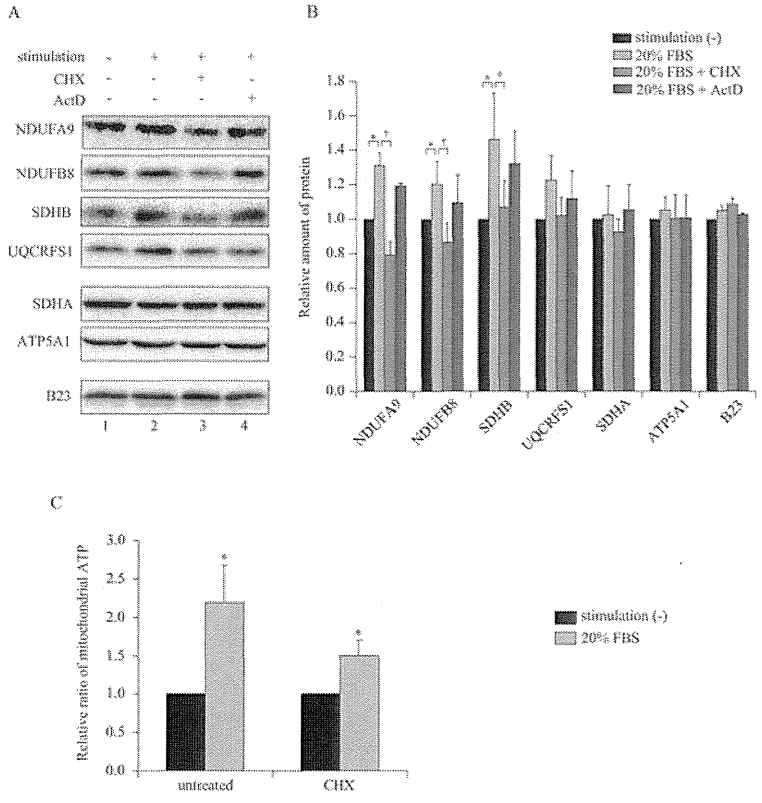

Figure 2 Serum stimulation regulates the expression levels of the nuclear-encoded OXPHOS proteins in a translation-dependent manner

(**A**) HeLa cells were cultured for 18 h in serum-free medium and then treated with 20 μg/ml CHX or 200 ng/ml ActD for 6.5 h. Stimulation with 20 % (v/v) FBS was carried out for 6 h. The cells were lysed and analysed by immunoblotting with antibodies against the indicated proteins. (**B**) The intensities of the signals in (**A**) were analysed by densitometry. $*P < 0.05$, stimulation (−) compared with 20 % (v/v) FBS and $\dagger P < 0.05$, 20 % (v/v) FBS stimulation compared with 20 % (v/v) FBS + CHX by Student's *t* test. There are no differences between experiments using 20 % (v/v) FBS and 20 % (v/v) FBS + ActD. (**C**) HeLa cells were cultured for 18 h in serum-free medium and later treated with 20 μg/ml CHX for 6.5 h and stimulated with 20 % (v/v) FBS for the last 6 h. The mitochondrial ATP levels were measured using chemiluminescence. The results shown were obtained from three independent experiments and are means ± S.D. $*P < 0.05$, stimulation (−) compared with 20 % (v/v) FBS by Student's *t* test.

Oxygen consumption assay

Oxygen consumption was measured as described previously [25]. HeLa cells were trypsinized, washed twice with PBS and permeabilized with respiration buffer [20 mM Hepes/KOH, pH 7.1, 2 mM potassium phosphate, 250 mM sucrose, 10 mM $MgCl_2$, 1 mM ADP and 1 % (v/v) digitonin]. The permeabilized cells were placed in the reaction chamber of a Clark-type electrode (Hansatech), and the oxygen concentrations were measured in a 1 ml volume at 37 °C with substrates and inhibitors according to standard protocols [26]. After addition of 5 mM glutamate and 5 mM malate, the oxygen concentration was monitored for 3 min before the reaction was inhibited by addition of 100 nM rotenone. After addition of 5 mM G3P (glycerol 3-phosphate) and 5 mM succinate, the oxygen concentration was monitored for 3 min before the reaction was inhibited by addition of 10 nM antimycin A.

RESULTS

Serum stimulation up-regulates nuclear-encoded mitochondrial proteins and mitochondrial ATP

Growth stimuli up-regulate mitochondrial functions, such as ATP production and oxygen consumption, by increasing protein expression [22]. To investigate whether serum stimulation regulates ATP production through transcription or translation, we examined the changes of OXPHOS proteins in response to serum stimulation by immunoblotting. HeLa cells were cultured in serum-free medium for 21 h and later stimulated by 20 % (v/v) FBS for 3 h. After the stimulation, the expression levels of NDUFA9, NDUFB8, SDHB and UQCRFS1 proteins were increased by approximately 30 %, whereas SDHA and ATP5A1 protein expression levels showed no change (Figures 1A and 1B). To confirm that the mRNA levels were not induced after serum stimulation, we performed qRT–PCR analyses on RNA isolated after serum stimulation. Unlike the protein levels, serum stimulation had little effect on the mRNA expression levels (Figure 1C).

Next, we examined whether serum stimulation affected ATP synthesis. The ATP levels were assessed by splitting into glycolytic and mitochondrial ATP production after 4 h of serum stimulation (Figure 1D). The serum stimulation significantly elevated only mitochondrial ATP, suggesting that serum stimulation up-regulates mitochondrial ATP production.

Serum stimulation regulates the expression of nuclear-encoded mitochondrial proteins in a translation-dependent manner

To assess whether the changes in response to serum stimulation are mediated by translational or transcriptional regulation, we added CHX (cycloheximide), a translational inhibitor, or ActD (actinomycin D), a transcriptional inhibitor, 30 min before adding serum and investigated the changes in protein expression. The increased expression levels of NDUFA9, NDUFB8 and SDHB to serum stimulation were completely suppressed by CHX treatment, but largely unaffected by ActD treatment (Figures 2A and 2B). The expression levels of SDHA and ATP5A1, which

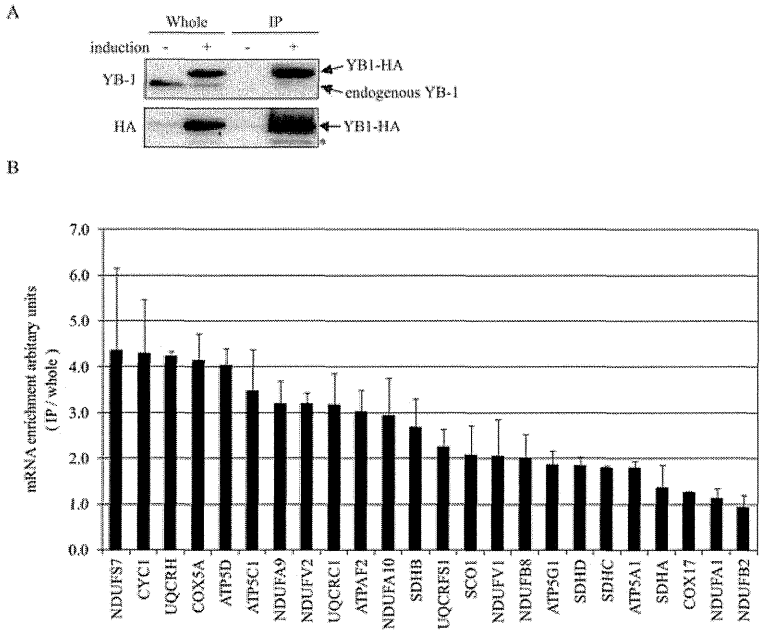

Figure 3 YB-1 associates with nuclear-encoded OXPHOS mRNAs

(**A**) HeLa/FRT/Tet-on cells were transfected with a YB-1–HA expression vector. YB-1–HA expression was induced by doxycycline for 48 h. The cells were lysed and subjected to immunoprecipitation with anti-HA agarose beads. The immunoprecipitated proteins (IP) and whole cell lysates were analysed by immunoblotting with anti-YB-1 or anti-HA antibodies. The asterisk indicates a non-specific band. (**B**) RNA was extracted from the immunoprecipitates and total cell lysate, then the mRNA levels were analysed by qRT–PCR. The ratio of each mRNA in the immunoprecipitant by YB-1 to the amount of total cell lysate is indicated. The results shown were obtained from three independent experiments and are means ± S.D.

showed no change in response to serum stimulation, were also unaltered by CHX or ActD treatment. These findings suggest that serum stimulation regulates the expression of nuclear-encoded OXPHOS proteins in a translation-dependent manner.

To determine whether ATP production in response to serum stimulation depends on translation, CHX was added 30 min before adding serum, similar to the experiments for the protein expression. Mitochondrial ATP production was increased 2-fold in response to serum stimulation in untreated cells, whereas CHX treatment suppressed the elevation after stimulation by 50 % (Figure 2C). These observations suggest that ATP production in response to serum stimulation mediates the increases in the nuclear-encoded OXPHOS proteins by translational regulation.

YB-1 associates with nuclear-encoded mitochondrial mRNAs

Previously, YB-1 was reported to associate with mRNA in polysomes or free mRNPs, and to act as either a translational activator or inhibitor, depending on the amount bound to target mRNA [14,15]. Therefore we hypothesized that YB-1 binds to the nuclear-encoded OXPHOS mRNAs and regulates their translation. To assess whether YB-1 associated with the nuclear-encoded OXPHOS mRNAs, RNA immunoprecipitation assays were performed in HeLa cells. We produced stable cell lines expressing recombinant full-length YB-1 with a C-terminal HA tag (YB-1–HA) upon induction by addition of doxycycline. The recombinant YB-1–HA was only observed in cells with added doxycycline for 48 h (Figure 3A). After immunoprecipitation with anti-HA antibodies from doxycycline-induced or non-induced cells, the proteins and RNAs were purified from immunoprecipitates. The precipitated RNAs and total RNAs were subjected to qRT–PCR (Figure 3B) and we compared the relative amount of immunoprecipitated mRNAs with their relative total amount in the cell. The ratio of mRNA immunoprecipitated compared with total RNA in the cell ranged 4-fold between *NDUFB2* and *NDUFS7* mRNA. We separated two mRNA groups with high or weak association with YB-1 protein. *NDUFA9* and *SDHB* mRNAs, whose translation was regulated by serum stimulation, were included in the high YB-1-associated group, whereas *SDHA* and *ATP5A1* mRNAs, which translation was not regulated by serum stimulation, were included in the weak YB-1-associated group. These findings suggested that high YB-1-associated mRNAs such as *NDUFA9* and *SDHB* were regulated at the translational level after serum stimulation, and that YB-1 is a key mediator for serum stimulation-mediated translational activity.

YB-1 regulates the translation of nuclear-encoded mitochondrial mRNAs by its concentration

YB-1 functions as either a translational activator or inhibitor depending on the amount binding to the target mRNA [27]. Therefore we investigated the mitochondrial proteins in HeLa cells after YB-1 depletion or overexpression. YB-1 protein was effectively depleted at 72 h after YB-1 siRNA transfection (Figure 4A). The expression levels of NDUFA9, NDUFB8, SDHB and UQCRFS1 proteins were increased by approximately 50 % after YB-1 depletion (Figures 4A and 4B). However, the expression levels of SDHA and ATP5A1 proteins, whose expression was not regulated by serum stimulation, were not altered after YB-1 depletion. The expression levels of COX2 (cytochrome *c* oxidase subunit 2), which is encoded by mtDNA, and nuclear protein B23 were not changed after YB-1 depletion. In contrast, YB-1 overexpression resulted in decreased expression levels of NDUFA9, NDUFB8, SDHB and UQCRFS1 proteins (Figures 4C and 4D). Thus far, the proteins encoded by mRNAs that tended to associate strongly with YB-1 were affected by the amount of YB-1 (Figures 3, 4B and 4D). NDUFA9 reacted sensitively to YB-1 depletion, but mildly to YB-1 overexpression.

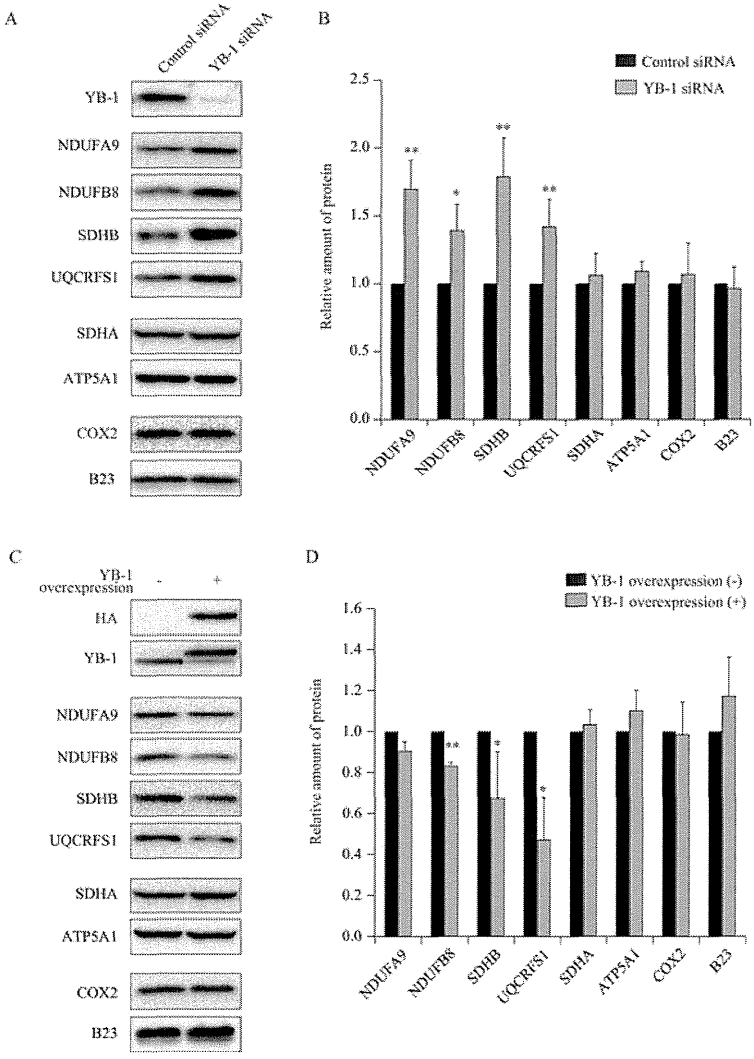

Figure 4 YB-1 depletion or YB-1–HA overexpression affects the translation levels of nuclear encoded OXPHOS mRNAs

(**A**) HeLa cells were transfected with a non-targeted (control) or YB-1 siRNA using Oligofectamine™. At 3 days after transfection, the effects of YB-1 depletion were analysed by immunoblotting with antibodies against the indicated proteins. (**B**) The intensities of the signals in (**A**) were analysed by densitometry. (**C**) Overexpression of YB-1–HA was induced by doxycycline for 48 h. The levels of the indicated proteins were analysed by immunoblotting. (**D**) The intensities of the signals in (**C**) were analysed by densitometry. The results shown were obtained from three independent experiments and are means ± S.D. $^{*}P < 0.05$ and $^{**}P < 0.01$ by Student's *t* test.

This raises the possibility that *NDUFA9* mRNA binds to YB-1 protein sufficiently to inhibit its translation at the steady-state condition. These observations suggest that YB-1 binds to a part of the nuclear-encoded OXPHOS mRNAs and regulates their expression at the translational level.

YB-1 regulates the recruitment of mRNAs from mRNPs to polysomes

It has been suggested that mRNAs exist in the state of translation-off, as mRNPs in the cytoplasm after export from the nucleus [28]. YB-1 is a major component of mRNPs [14] and inhibits protein synthesis at the initiation stage. To examine whether YB-1 regulates the synthesis of the nuclear-encoded OXPHOS proteins at the translation initiation stage, we analysed the sedimentation profiles in a sucrose density gradient. HeLa cells were cultured for 72 h after YB-1 siRNA transfection and the post-nuclear supernatant was centrifuged on a 15–45 % (w/v) sucrose gradient. Immunoblotting analysis showed that YB-1 protein was contained in all fractions in control siRNA-transfected cells, but was hardly detected in YB-1 siRNA-mediated knockdown cells. S6 ribosomal protein was detected in fractions 7–16, with the majority in fractions 10–12 (Figure 5A). Phosphorylated eIF (eukaryotic initiation factor)-4E, as a translation initiation complex marker, was mainly found in fractions 7–9 (Figure 5A). However, the distributions of S6 ribosomal protein and phospho-eIF-4E showed no change after YB-1 depletion. qRT–PCR analysis showed that 18S rRNA was contained in fractions 7–16, mostly similar to S6 protein, and 28S rRNA was distributed in fractions 9–16 (Figure 5B). The rRNA distributions showed no change after YB-1 depletion, similar to the ribosomal proteins.

We defined the mRNAs in fractions 5–8 as translationally inactive mRNAs and those in the fractions 12–16 as translationally active mRNAs, as described previously [29]. The ratios of *NDUFA9* and *SDHB* mRNAs in the inactive mRNA fraction were decreased, whereas those in the active mRNA fraction were increased after YB-1 depletion. YB-1 depletion did not change the ratio of inactive and active *ATP5A1* mRNA (Figure 5B).